A THESIS SUBMITTED TO
THE GRADUATE SCHOOL OF NATURAL AND APPLIED SCIENCES
OF ÇANKIRI KARATEKİN UNIVERSITY

PRODUCTION AND INVESTIGATION OF ANTIBACTERIAL PROPERTIES OF DOPED Sn-Cu ZnO THIN FILMS

IN PARTIAL FULFILLMENT OF THE REQUIREMENTS
FOR THE DEGREE OF MASTER OF SCIENCE
IN PHYSICS

BY

NOORALHUDA KAREEM HANOON ALHUSSEINAWI

ÇANKIRI

2023

PRODUCTION AND INVESTIGATION OF ANTIBACTERIAL PROPERTIES DOPED Sn-Cu ZnO THIN FILMS

Nooralhuda Kareem Hanoon ALHUSSEINAWI

February 2023

We certify that we have read this thesis and that in our opinion it is fully adequate, in scope and in quality, as a thesis for the degree of Master of Science

Advisor **:** Asst. Prof. Dr. İlker KARA

Examining Committee Members:

Chairman **:** Prof. Dr. Özcan YALÇINKAYA
Department of Chemistry
Gazi University

Member **:** Assoc. Prof. Dr. Olcay GENÇYILMAZ
Department of Material and Material Processing Technologies
Çankırı Karatekin University

Member **:** Asst. Prof. Dr. İlker KARA
Department of Medical Services and Techniques
Çankırı Karatekin University

Approved for the Graduate School of Natural and Applied Sciences

Prof. Dr. İbrahim ÇİFTÇİ
Director of Graduate School

I hereby declare that all information in this document has been obtained and presented in accordance with academic rules and ethical conduct. I also declare that, as required by these rules and conduct, I have fully cited and referenced all material and results that are not original to this work.

Nooralhuda Kareem Hanoon ALHUSSEINAWI

ABSTRACT

PRODUCTION AND INVESTIGATION OF ANTIBACTERIAL PROPERTIES OF DOPED Sn-Cu ZnO THIN FILMS

Nooralhuda Kareem Hanoon ALHUSSEINAWI

Master of Science in Physics

Advisor: Asst. Prof. Dr. İlker KARA

February 2023

Today, ZnO (zinc oxide) based semiconductor samples, which have great potential, are the most frequently preferred materials to develop devices based on nanotechnology. It is also used in studies due to its excellent chemical stability, biological non-toxicity, and low cost. In this study, undoped thin films and Sn-Cu doped ZnO thin films at different concentrations were grown on FTO substrates by using the SILAR method. Undoped ZnO thin films and Sn-Cu doped thin films were accumulated on the FTO substrate in different concentrations 40 times, and then they were annealed at 300 °C. Properties, which are structural, surface morphological, antibacterial properties, bacterial adhesion, and survival organism count, of undoped thin films and Sn-Cu doped thin films were investigated by using SEM-EDS, the agar diffusion test, and the organism counting method. From the SEM-EDS analysis, it was observed that both undoped and doped films with different Sn-Cu concentrations enlarged harmoniously on the FTO substrate. Their morphological properties changed depending on the doping concentration. It was observed that the produced samples did not show antibacterial activity. The highest adhesion rate of bacterial organisms on the produced samples was observed when the ZnO/Sn-Cu doping rate was 3 %. In addition, the lowest adhesion rate was observed when the ZnO/Sn-Cu additive ratio was 1 %.

2023, 69 pages

Keywords: SILAR method, Zinc oxide, Thin films, Agar well diffusion

ÖZET

Cu-Sn KATKILI ZnO FİLM ÜRETİMİ VE ANTİBAKTERİYEL ÖZELLİKLERİNİN İNCELENMESİ

Nooralhuda Kareem Hanoon ALHUSSEİNAWİ
Fizik, Yüksek Lisans
Tez Danışmanı: Dr. Öğr. Üyesi İlker KARA
Şubat 2023

Günümüzde nanoteknolojiyi temel alan cihazların geliştirilmesinde, büyük bir potansiyele sahip olan ZnO (Çinko oksit) temelli yarıiletken numuneler en sık tercih edilen malzemelerdendir. Ayrıca mükemmel kimyasal stabilitesi, biyolojik olarak toksik olmaması ve düşük maliyeti nedeniylede çalışmalarda kullanılmaktadır. Bu çalışmada katkısız ve farklı konsantrasyonlarda Sn-Cu katkılı ZnO ince filmler FTO alltaş üzerine SILAR yöntemi kullanılarak büyütülmüşlerdir. Farklı konsantrasyonlar 40 kat olacak şekilde FTO alttaş üzerine biriktirilen ve sonrasında 300 °C'de tavlanan katkısız ve Sn-Cu katkılı ince filmlerin yapısal, yüzeysel morfolojisi, antibakteriyel özellikleri, bakteriyel yapışma ve hayatta kalma organizma sayımı özellikleri SEM-EDS, agar difüzyon testi ve organizma sayma yöntemi kullanılarak incelenmiştir. SEM-EDS analizlerinden katkısız ve farklı konsantrasyonlarda Sn-Cu katkı konsantrasyonuna bağlı olarak üretilerin filmlerin FTO alltaş üzerine uyumlu birşekilde büyüdüğü ve katkı konsantrasyonuna bağlı olarak morfolojik özelliklerinin değiştiği gözlendi. Üretilen numuneler antibakteriyel etkinlik göstermediği görülmüştür. Üretilen numuneler üzerine bakteri organizmalarının yapışma oranı en yüksek ZnO/Sn-Cu %3 katkılı numunede en düşük oran ise ZnO/Sn-Cu %1 katkılı numunede görülmüştür.

2023, 69 sayfa

Anahtar Kelimeler: SILAR metot, Çinko oksit, İnce film, Agar kuyu difüzyonu

PREFACE AND ACKNOWLEDGEMENTS

I would like to thank my thesis advisor, Asst. Prof. Dr. İlker KARA, for his patience, guidance and understanding.

Nooralhuda Kareem Hanoon ALHUSSEINAWI
Çankırı-2023

CONTENTS

LIST OF SYMBOLS

A	Absorbance value
α	Absorption coefficient
Å	Angstrom value
β	Half peak width
°C	Centigrade degree
Cs	Crystal size
d_{hkl}	Interplaner distance
d_{XRD}	Experimental distance
d_{CARD}	Standard distance
E_g	Energy gap
E_{ph}	Phonon energy
eV	Electron volt
h	Planck's constant
I	Transmittance intensity
I_A	Absorbed intensity
I_R	Reflected intensity
I_o	Standard intensity
K	Shape factor
k	Extinction coefficient
k_B	Boltzman constant
λ	Wavelength value
M	Molar value
$M_{(hkl)}$	Miller indices
nm	Nanometer value
n_o	Refractive index
N	Complex refractive index
R	Reflectance value
δ	Dislocation density
ν	Frequency value
T	Transmittance value
TCO	Transparent conductive oxides
θ	Bragg angle

LIST OF ABBREVIATIONS

EDS	Energy dispersive X-ray spectroscopy
FESEM	Field emission scanning electron microscope
UV-VIS	Ultraviolet-visible
XRD	X-ray diffraction

LIST OF FIGURES

LIST OF TABLES

1. INTRODUCTION

In general, nanoparticles are small pieces of matter with a diameter of 1 - 100 nm. According to that definition, nanoparticles are in the same size range as airborne ultrafine particulates and are a subset of colloidal particles (Christian *et al*. 2008). In the last 20 years, scientists proved that nanoparticles could be found anywhere in the environment (Klapiszewska *et al.* 2022).

Scientists put nanoparticles into different groups based on their shape, size, and chemical properties. The main types of nanoparticles are carbon-based nanoparticles, metal nanoparticles, ceramic nanoparticles, semiconductor nanoparticles, and polymeric nanoparticles (Khan *et al.* 2019). Nanotechnology or nanoparticle technology is the science that studies how to treat matter at the atomic and molecular levels. Nanotechnology is about making new technologies and methods whose sizes are measured in nanometers (Mashaghi *et al.* 2013).

Most of the time, nanotechnology works with groups of 5 to 1000 atoms. These clusters are much smaller than living cells and bacteria. This technicality has nothing to do with biology. Instead, it's about the properties of nanomaterials.

Nanotechnology interacts with any phenomenon or building at the nano-level, so figuring out how to measure is important because of how the materials used change. Nanoparticles like these can cause a quantum confinement effect, which can lead to new electromagnetic and optical properties of matter. Nanoscience is one of the fields of material science, and it is linked to mechanical engineering, bioengineering, physics, and chemical engineering. All of these fields are interested in studying the properties of matter at this small scale (Goncharova *et al.* 2018).

Nanotechnology's main challenge is dominating atoms after splitting their materials. They need sensitive size, measurement, and vision devices to check for particles. When measuring at the atomic level, it's difficult to be precise. Nanotechnology's impact and need to be mastered are still debated (Blair *et al*. 2014).

Nanotechnology is a branch of science that combines nanoscience and biotechnology to produce, process, and design new functional nanomaterials to deliver drugs to targeted tissues, release them at a controlled rate, and sometimes escape degradation in the body (Patra *et al.* 2018).

Researchers are interested in using nanotechnology to build and modify materials at the nanoscale to create unique metal-oxide nanostructures. Metal-oxide nanostructures such as nanorods, nanowires, and nanotubes have been studied for biochemical and biological applications. Biosensing, biological separation, molecular imaging, biomarkers, and cancer therapy are examples. Their high surface-to-volume ratio, ability to have surfaces customised, biosafety, and biocompatibility open up new biomedical potential. Nanostructures are being used to produce electrochemical intracellular biosensors. A material with a metal-oxide nanostructure and exciting surface-charge characteristics can be used to integrate biorecognition elements with a signal amplifier. These nanostructures are functional, biocompatible, nontoxic, and catalytic. They exhibit high electron-transfer kinetics and long-lasting adsorption, which makes them ideal for immobilising biomolecules and enhancing biosensing.

Zinc oxide (ZnO), which is one of the best metal-oxide semiconductors, is also generally biosafe and biocompatible, making it appropriate for use in applications involving intracellular sensors and transducers (Islam *et al.* 2022, Collares *et al.* 2020, Amendola *et al.* 2020).

When it comes to curing bacterial illnesses, antibiotics are now considered the gold standard (Davies and Davies 2010). The problem is that bacteria and viruses can become immune to antibiotics. Most pathogenic bacteria can become resistant to at least some classes of antibiotics. Bacterial antibiotic resistance can be attained in a number of ways, including by inhibiting the uptake of antibiotics by cells (Kumar and Schweizer 2005, Blair *et al.* 2014) altering the antibiotic's target (Reygaert 2009, Randall *et al.* 2013) deactivating the drug using enzymes (Blair *et al.* 2015, World Health Organization 2015) or actively excreting it (Kumar and Schweizer 2005).

Infections of the digestive tract and lungs are among the top 10 causes of death and disability, according to World Health Organization (WHO) statistics in 2015. The prevalence of fatal bacterial infections and the frequency with which people died from them both skyrocketed with the emergence of antibiotic-resistant strains. Antibiotic-resistant bacterial species are now responsible for more human fatalities than both cancer and diabetes combined. Antibiotic resistance was proven despite the availability of a large number of different drugs. Shortly after a new antibiotic is licenced for use, resistant bacteria begin to evolve. Because of what has transpired, WHO in 2015 (endorsed the Global action plan on antimicrobial resistance). Bacterial co-infection and secondary infection are common in patients with COVID-19 and can contribute to higher mortality among critical care unit patients. With these factors in mind, it is clear that the quest for novel antimicrobial treatments should be a top priority for public health organisations throughout the globe.

Between 2018 and 2020 alone, there will be over 99000 scholarly articles devoted to the study of potential new antimicrobial compounds, with approximately 5900 of those articles specifically focusing on the study of potential new antibacterial compounds based on metal compounds (Collares *et al.* 2020).

Nanotechnology is the most important area of active research in material science right now (Islam *et al.* 2022). Nanotechnology has grown a lot, as shown by the number of scientific articles about it and the many ways it can be used (Collares *et al.* 2020). Scientists all over the world have recently shown interest in making metal and metal oxide nanoparticles (NPs) (Amendola *et al.* 2020). ZnO-NPs are very important because they can be used in many different ways, such as in photocatalysis, water purification, and killing bacteria. ZnO-NPs are different from other NPs in how they behave (Llama-Palacios *et al.* 2019). ZnO-NPs have biological effects that depend on their size and shape, which are being looked into by many researchers (Collares *et al.* 2020, Klapiszewska *et al.* 2022, Husain *et al.* 2022, Abdelmigid *et al.* 2022). ZnO-NPs are thought to be useful for many things, and in recent years, researchers have been focusing on these metallic NPs because they are very good at killing bacteria (Qi *et al.* 2016, Ahmadian *et al.* 2018).

The ability of these nanostructured agents to kill bacteria is due to their high surface-to-volume ratio, which gives them a bigger area to interact with bacteria in the environment. Being able to easily get through cell membranes upsets many processes inside the cell, leading to a high level of reactivity and antibacterial activity (Tülü *et al.* 2021, Song and Ge 2019).

Special attention has been paid to the use of ZnO in dental parts because it is an effective alternative for biomedicine, especially for oral health. Gram-negative bacteria such as Escherichia coli are susceptible to the antibacterial capabilities of ZnO as a nanocomposite (*E. coli*) (Jiang *et al.* 2016, Chinnapaiyan *et al.* 2022) as well as Gram-positive bacteria like Enterococcus faecalis (*E. faecalis*) and Staphylococcus aureus (*S. aureus*), and it has become popular for getting rid of these bacteria from the mouth (Collares *et al.* 2020, Klapiszewska *et al.* 2022, Husain *et al.* 2022).

1.1 Literature Review

Nanotechnology is a new research technique. The primary principles underlying it predate the technology. Taniguchi (1974) initially introduced the word "nanoparticle" in 1974 to describe semiconductor techniques like thin-film deposition and ions beam milling. Most living things are nanoscale, hence nature is full of nanomaterials. As stated in the introduction, NPs intend to manufacture and use both novel and natural nanomaterials in bigger volumes and within consistent size ranges (Doyle 2006).

In 2018, investigate the antibacterial, chemical, and physical characteristics of ZnO nanoparticles produced by pulsed laser ablation in air and water (Goncharova *et al.* 2018). Gram-positive Staphylococcus aureus was used to evaluate the nanoparticles' antibacterial efficacy (*S.aureus*). Ablation conditions were shown to affect the physical and chemical antibacterial properties of nanoparticles. ZnO nanoparticles were then applied to the models. Using a scanning electron microscopy technique, we examined the model bandage materials for antibacterial activity in accordance with ISO 20743:2013. When tested against S.aureus, all of the compounds performed quite well.

In 2019, zinc oxide nanoparticles (ZnO NPs) have received a lot of interest recently due to their unusual features (Mohd Yusof *et al.* 2019). Notably, research suggests that zinc is an essential mineral for living organisms. As a result, both prokaryotes and eukaryotes, including bacteria, fungus, and yeast, are used to synthesise ZnO NPs via intracellular or extracellular microbial cells, enzymes, proteins, and other molecular components. ZnO NPs have antibacterial capabilities; however, the properties of nanoparticles (NPs) are dependent on their size and form, making them suitable for a variety of applications. However, the ideal size and form the optimization method of microbe-mediated synthesis can yield NPs by altering their reaction conditions. It should be mentioned that ZnO NPs are created using a variety of chemical and physical processes.

Nonetheless, these technologies are costly and harmful to the environment. As a result, microbe-mediated synthesis of ZnO NPs has lately progressed significantly, with the microorganisms being cleaner, eco-friendly, non-toxic, and biocompatible as alternatives to chemical and physical methods. Furthermore, zinc in the form of NPs is used. Because they are more effective than their bulk equivalents, they have been investigated for a wide range of prospective uses.

Criteria for the optimization process and their prospective employment as an antibacterial agent and feed additive in the animal business, as well as their toxicological dangers to animals.

In 2020, Metal oxide nanoparticles have unique physicochemical properties that make them a possible antibiotic alternative (Sharma *et al.* 2020). Bacterial infection causes most human illnesses. Antibiotics are used, but they have other side effects. This study aims to determine the antibacterial effects of ZnO and Ag nanoparticles on Escherichia coli as a model bacterium. Bacterial infection causes most human illnesses. Antibiotics are used, but they have other side effects. This study aims to determine the antibacterial effects of ZnO and Ag nanoparticles on Escherichia coli. Surfactant-mediated nanoparticle creation takes one or two processes. CTAB and hydrazine hydrate are used. X-ray diffraction, scanning electron microscopy, and energy dispersive X-ray

spectroscopy study nanoparticle structure, shape, and content. Antibacterial nanoparticles are also tested using agar-well diffusion. The created nanoparticles are circular, 6 nm and 13 nm, and contain the necessary elements. Nanoscale ZnO/Ag particles killed *E. coli*. ZnO and Ag metal oxide nanoparticles have better antibacterial activity against *E. coli*, suggesting they could cure bacterial and fungal illnesses.

In 2021, Onto warmed glass, ZnO thin films with varied Al/Zn ratios were produced to be highly c-axis oriented and have a wurtzite structure using spray pyrolysis (Ali *et al.* 2021). More than 90 % of visible light was transmitted through these films, and colour bands seen at an off-angle indicated a high-quality surface. When the Al/Zn ratio was increased, the surface morphology suddenly shifted from a combination of nanorods and hexagonal stacks to a pyramidal one. Adding Al to the ZnO lattice caused the optical band gap to shift upwards toward high photon energies, which was thought to be a result of the Burstein-Moss effect. Defects and oxygen vacancies associated with zinc were detected using photoluminescence spectroscopy. The antibacterial activity of the films was evaluated against Escherichia coli bacteria, and it was found to increase with a higher Al/Zn ratio. Surgical tools, protective hospital garb, medical implants, storage containers, textiles, and food packaging could all benefit from these antimicrobial coatings' exceptional optical qualities.

In 2022, pure and Al doped ZnO thin films were fabricated using a two step SILAR procedure (Shankar Ganesh *et al.* 2022). Pure ZnO thin film and ZnO thin film doped with Al (1 %, 3 %, and 5 %) were studied for their structural, optical, and morphological characteristics. All of the diffraction peaks from this sample fit neatly into a hexagonal Wurtzite crystal structure. Dislocation density, crystallite size, microstrain, and lattice parameters were all determined for the artificial thin films. When it comes to morphology, pure ZnO thin films are spherical, while Al doped ZnO thin films take on a rod like structure with hexagonal faces. As the percentage of Al in the final thin film increases, its bandgap narrows. Photoluminescence (PL) studies verified the presence of dee-level and neaband edge emissions. *S. aureus* and *E. coli*, twogrammem-positive andgrammem-negative bacteria, were tested in agar diffusion experiment to determine their respective maximum zones of inhibition. Significant

antibacterial activity was observed for both pure and Al-doped ZnO. There is notable antibacterial activity in every one of the samples. Al-doped ZnO, XRD, FESEM, UV-VIS, and antimicrobial activity.

2. GENERAL THEORETICAL INFORMATION

2.1 Brief Overview of ZnO Characteristic

These characteristics make ZnO more resistant to wear (Özgür *et al.* 2005, Ferblantier 2005). The semiinsulating substrate enables direct electrical characterization of epitaxial films, particularly thin films, and inhibits parasitic currents in field effect transistors (Hussain 2008).

Evaluation of semiconductors one of the earliest pure semiconductors was ZnO, which came before silicon and germanium. In the 1950s and 1960s, its acoustoelectric and piezoelectric capabilities were investigated. In the ultraviolet (UV) and short wavelength regions of the electromagnetic spectrum, wide band gap semiconductors have attracted interest as optoelectronic components. Blue and UV LEDs and injection lasers were enhanced using ZnSe based devices and GaN based technology.

SiC's indirect band structure prevents it from emitting bright light, and ZnSe's high current drive causes defects. GaN is the best optoelectronic material. ZnO has advantages over semiconductors for LEDs and LDs. Due to its wide and direct band gab, ZnO as an II-VI semiconductor is promising for optoelectronic short wavelength light emitting devices.

The semiconductor that is most radiation-resistant is ZnO. ZnO devices benefit from this feature in high-energy radiation conditions and in space. Band gap energy may be raised by alloying from 3.3 to 4.5 eV. Therefore, it can be utilized in quantum well lasers and heterostructured LEDs. These distinctive nanostructures demonstrate that in terms of structure and characteristics, the ZnO family of nanostructures is the most diverse (Özgür *et al.* 2005).

2.2 The Basic Properties of Zinc Oxide

2.2.1. Crystal structure

Polar surfaces and a non-centrosymmetric wurtzite crystal structure are also features of ZnO. The wurtzite structure of ZnO can be thought of as being made up of two interlocking hexagonal close-packed (hcp) sublattices of cations (Zn) and anions (O) that are moved in the c-direction by the length of the cation-anion bond. The ZnO hexagonal unit cell has a lattice constant of a = 3.2500 and c = 5.2060. In an ideal wurtzite structure, each hexagonal close packed (hcp) unit is made up of atoms of the same type that are moved away from each other along the threefold c-axis by u = 3/8 = 0.375 in fractional coordinates. In an ideal wurtzite crystal, the bond angle is 109.070 Figure 2.1 shows this.

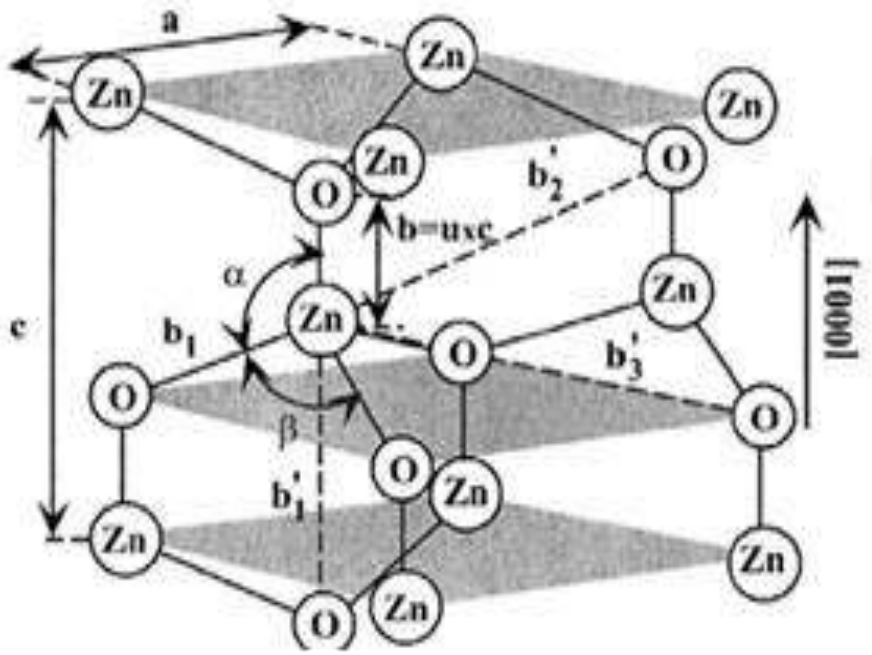

Figure 2.1 Schematic drawing of a wurtzitic ZnO structure (Özgür *et al.* 2005)

At the borders of a tetrahedron, each group-II atom is surrounded by four group VI atoms, or vice versa, and each sublattice has four atoms per unit cell. The c/a ratio or u value of real ZnO crystals is different from the ideal wurtzite structure. Wurtzite crystal

deviations may be caused by lattice stability and ionicity. In heteroepitaxial layers, the ZnO lattice constant goes up because of zinc antisites, oxygen vacancies, and threading dislocations.

If the following relationship holds, the lengths of these two bonds will be the same in Equation (2.1).

$$\mu = \left(\frac{1}{2}\right)\left(\frac{a^2}{c^2}\right) + \frac{1}{4} \tag{2.1}$$

2.2.2 Parameters of the lattice

ZnO has a significant degree of ionic bonding; as a result, the lowest unoccupied orbital (LUMO) in the conduction band and the highest unoccupied orbital (HOMO) in the valence band are created from the 4s levels of Zn^{2+} and the 2p levels of O_2 respectively.

The band gap for low-temperature conduction is 3.437 eV. Covalent chemical bonding and sp3 hybridization are present in the crystal structures of diamond, zinc blende, and wurtzite. Group IV semiconductors like diamond, silicon, and germanium have only covalent bonds.

When developing semiconductors, lattice parameters are important. Four factors determine the semiconductor lattice parameters. Free-electron concentration affects the conduction band potential. (ii) the difference in impurity concentration and ionic radius between substituted matrix ions. external strains (iii) temperature Lattice imperfections disrupt its strict periodicity. These flaws control semiconductors' mechanical, thermal, electrical, and optical properties. Plasticity, hardness, and thermal and electrical conductivities are determined. High-resolution X-ray diffraction measures lattice parameters of crystalline materials (HRXRD). Figure 2.1 compares ZnO lattice parameters measured and calculated by several groups. (Özgür *et al.* 2005). ((a), Determined by employing a technique known as X-Ray diffraction, (b) Determined

through the application of powder X-ray diffraction, (c) Determined through the application of the ab-initio periodic linear combination of atomic orbitals (LCAO) method).

2.2.3 Structure of an electronic band

The band structure of a semiconductor is a very important property because it determines important properties like the band gap and the effective electron and hole masses. In terms of device applications, band gap engineering, and UV lasing at room temperature, ZnO is regarded to be the semiconductor in its family that best fits these criteria. Because of this, it's crucial to comprehend the band structure in order to explain the electrical qualities and a variety of other things (Özgür *et al.* 2005, Hussain 2008).

ZnO's direct band gap is its most important property. The band structure has recently been computed using an empirical tight-binding Hamiltonian. The Brillouin zone symmetry lines provide the ZnO band structure E_k. The band gap between occupied and empty bands (1 and 5.1) is important. ZnO's Eg is 3.3 eV. The energy difference between full and empty (Figure 2.2). ZnO is called a direct band gap semiconductor because the edges of the valence band and the conduction band are at the same k values (Göpel 1982).

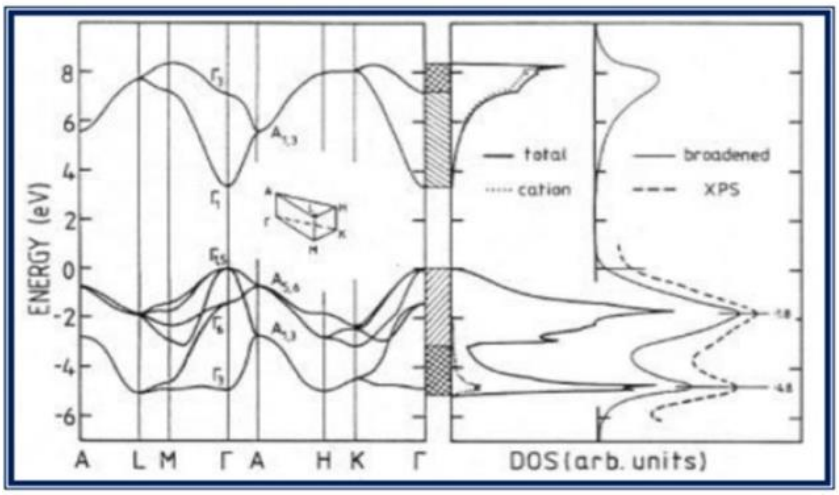

Figure 2.2 Shows six valence bands between -6 and 0 eV

2.2.4 Optical properties

Semiconductor optical properties are intrinsic and extrinsic. Excitonic effects due to the Coulomb interaction occur between conduction band electrons and valence band holes. For exciton formation, equal electron and hole group velocity is required. ZnO is a transparent conductive material with a direct bandgap semiconductor, as we have already explained. Depending on the carrier concentration, the plasma edge of ZnO films lies between 2 and 4 m in wavelength range between 0.3 and 2.5 m. It is well knowledge that when carrier concentration rises, the band gap edge shifts. Burstein-Moss shift is the name given to this shift. The near UV-band is directly tied to the material's excitonic nature and can coexist with biexciton emission as well as free exciton emission and its phonon copy. Even at low temperatures, it is typically difficult to observe light from exciton. There are several causes for this (Stoimenov *et al.*2002).

2.2.5 Electrical properties

Due to its wide band gap and high exciton binding energy of 60 meV, ZnO is a direct semiconductor that is particularly intriguing for optoelectronic and electrical devices. A device built from a material with a bigger band gap, for instance, may have a high breakdown voltage, produce less noise, operate at higher temperatures, and use a lot of power.

The path taken by electrons through a semiconductor varies depending on the electric field strength. At low electric fields, ZnO electrons don't get much energy from the applied field compared to their thermal energy. Because the scattering rate doesn't change much, electron mobility will be constant.

As the electrical field is increased, the electrons' electrical energy equals their thermal energy. From equilibrium, the electron distribution function changes significantly. These electrons become hot, hotter than the lattice. The lattice doesn't lose any energy for a brief, crucial period (Hussain 2008).

2.2.6 ZnO doping defects

In recent years, wide bandgap semiconductors have received much attention due to their potential as blue light emitting devices, short-wavelength laser diodes, and UV-blue detectors. To reach ZnO's potential, high-quality n- and p-type ZnO is needed. In wide-bandgap semiconductors like GaN and II-VI compounds like ZnS, ZnSe, and ZnTe, bipolar carrier doping (both n and p types) is difficult. Unipolar doping in wide-bandgap semiconductors is not surprising: ZnO, GaN, ZnS, and ZnSe are easy to n-type dope, but p-type doping is difficult (Figure 2.3.).

Undoped ZnO is n-type, with donor concentrations around 10^{17} cm^3 for high-quality material but as high as 10^{21} cm^3 for doped material. Figure 2.3 shows the main single-crystal ZnO defect types, but none are shallow. X isn't a foreign atom. Zn on O antisites occur (Hussain 2008).

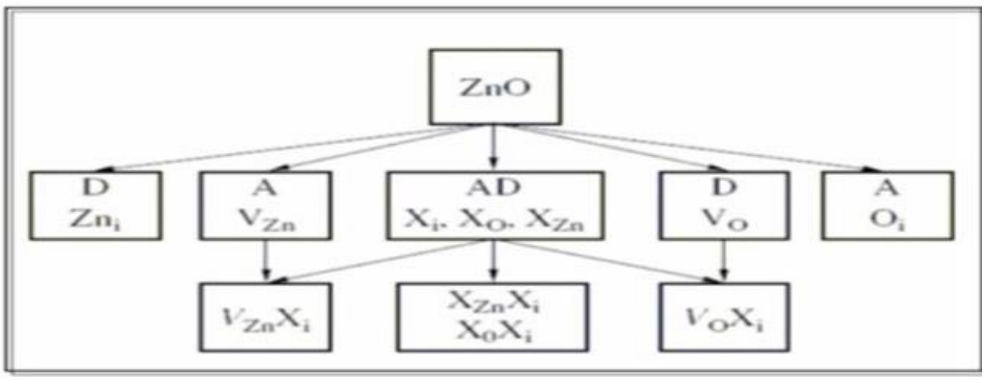

Figure 2.3 List of the different types of flaws that can happen in ZnO

n-type doping

Wurtzite is how ZnO is made, and ZnO always has too much zinc. ZnO is not a stoichiometric compound because it has too much zinc. It is an n-type semiconductor. Undoped ZnO has high electron densities of about 10^{12} cm^{-3} and n-type conductivity.

Interstitials of zinc In an unintentional ZnO film, the most important native donors are known to be ZnI and the oxygen vacancy Vo.

Hydrogen (H), a shallow donor with 31 meV activation energy, may be responsible for unintentionally doped ZnO film's n-type conductivity, not ZnI. Hydrogen (H) diffuses easily into ZnO in all growth methods.

ZnO n-doping is easier than p-doping. Al, Ga, and In can replace Zn as n-type dopants, and Cl and I can replace O. Doping with Al, Ga, and In has resulted in high-quality, conductive ntype ZnO films (Özgür *et al.* 2005).

p-type doping

Wide-bandgap semiconductors are difficult to p-dope. Lattice defects and impurity atoms can be ZnO acceptors. ZnO acceptors include Oi and Vzn. Deep impurity levels can also cause doping problems by preventing shallow acceptor formation.

Li, Na, and K are shallow acceptors on Zn sites, while N, P, and As are deep acceptors on O sites. Group-I participants are shallower than group-V. Larger Na and K bond lengths than the ideal Zn-O bond length (1.93A) induce lattice strain, forming vacancies to compensate shallow dopants (Park *et al.* 2002).

P and As have longer bonds than N in Group V (N, P, As). To avoid lattice strain, they form antisites (Özgür *et al.* 2005).

2.3. Characterization Techniques

2.3.1 Diffraction of X-rays by powder

A non-destructive method for analyzing crystalline materials is X-ray diffraction (Hussain 2008). X-rays are short-wavelength electromagnetic waves and particles with

a lot of energy. Photon energy (E), wavelength (the distance between peaks), and frequency can all be used to describe them (the number of peaks passing a point in a unit of time). Energy, frequency, or wavelength of a photon in Equation (2.2).

$$E = hv = \frac{hc}{\lambda} \tag{2.2}$$

When the values of the constants above are put into the in Equation (2.3), the following relationship is found in Equation (2.3).

$$\lambda = \frac{12.4}{E(Kev)} \tag{2.3}$$

Any X-Ray tube must have a source of electrons, a high voltage that speeds up the electrons, and a metal target. When an electron beam and a target interact, energy is lost. When high-energy electrons hit the anode material more than once, they create a continuous spectrum, or Bremsstrahlung. The fast deceleration of electrons striking the target causes the continuous spectrum to develop, but not all electrons decelerate similarly. While some deflect as they come into contact with their target atoms, losing little amounts of their total kinetic energy until they are completely exhausted, others halt in one collision and release all of their energy at once. Maximum energy (wavelength) photons are created when two halted electrons collide (Hussain 2008).

2.3.2 Bragg's law

A diffracted beam is created when X-rays dispersed from a crystalline solid interact constructively with atoms. In 1912, W. L. Bragg discovered a predictable link (Figure 2.4). They are combined by Bragg's law in Equation (2.4).

$$n\lambda = 2d\sin\theta \tag{2.4}$$

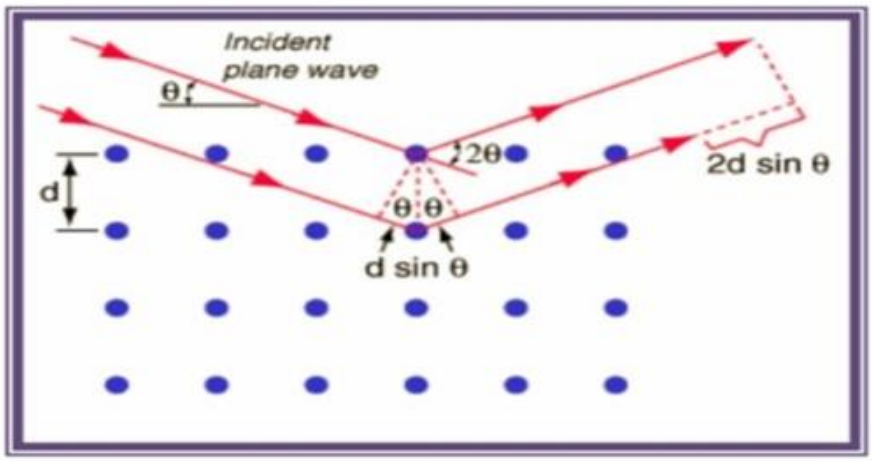

Figure 2.4 Bragg's diffraction condition

ƛ = the wavelength of the incoming X-radiation, which in our case is 1.54 angstroms and is represented by the Greek letter lambda.

d = the distance between two similar planes of atoms in a mineral, which is called the interatomic spacing and is measured in angstroms is the angle of diffraction in degrees = θ.

2.3.3 Measuring the size of a crystallite

When using x-ray diffraction to find out what phase something is in, the positions of the peaks in a diffraction profile and the relative strengths of these peaks are both important. Small grain size is another kind of flaw that can change the widths of the diffraction peaks. Broadening of peaks is caused by very small crystals. The size of a crystallite is easy to figure out based on its peak width, peak position, and wavelength.

2.3.4 Determination of the lattice parameters

The Miller indices hkl for the wurtzite structure connect the interplanar distance of the hkl plane to the lattice parameters a and c, in Equation (2.5).

$$\left(\frac{1}{d_{hkl}}\right)^2 = \frac{4}{3}\left(\frac{h^2 + k^2 + hk}{a^2}\right) + \frac{l^2}{c^2} \tag{2.5}$$

This is how you figure out the c lattice parameterand for the determination of a lattice from a second measurement d_hklof with either h or k different from zero.

2.3.5 Scanning electron microscopy (SEM)

Scanning Electron Microscopy (SEM) can give a high-magnification image of the surface of a material and information about its structure in surface areas. The resolution of SEM can be as small as a few nanometers, and it's easy to change the magnification from 10 times to 300,000 times (Randall *et al.* 2013).

Figure 2.5 shows a schematic of a model Scanning Electron Microscope (SEM) with different combinations. It is mostly made up of an electron gun, different electromagnetic lenses, an aperture, magnetic scanning coils, and different electron detectors. This is how SEM works at its most basic level. Emission beam electronic from the electron gun due to applying a voltage accelerated vertically during the anode attracted in electrons pass through several magnetic lenses before reaching the surface of the sample. The function of condenser lenses is to reduce the size of the electron beam, which in turn affects the resolution of the SEM (Khan *et al.* 2018).

Any undesired electrons cannot spray through the objective aperture. The beam is focused on the sample's surface by the functional objective lens, and the sample is moved over the specimen by scan coils in a raster pattern. As the electron beam hits the surface, it will create many signals in the form of electrons or photons. Emission signals from the specimen are picked up by detectors and turned into images.

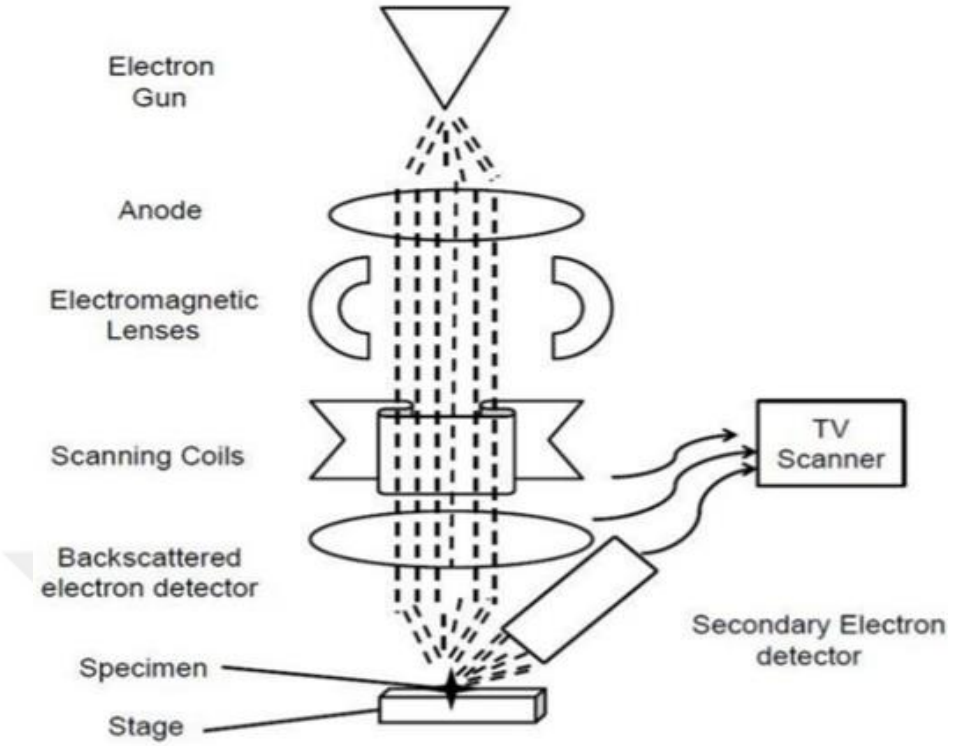

Figure 2.5 Typical of SEM (Tülü *et al.* 2021)

2.3.6 Transmission electron microscopy (TEM)

The highest melting point and lowest vapour pressure are found in a LaB6 or tungsten filament cathode, which is used as the cathode in a conventional transmission electron microscope (TEM). A point source is a small portion of the filament from which the electron beam is released. This point is important because it emits monchromatic electrons beam with an energy of 100 KV to 1 MKV. A positive potential is applied to the anode. Electrons are accelerated down the column by the cap's negative potential. Condenser lenses force electrons from a gun. The first lens determines the spot size, and the second lens changes it on the sample to restrict the electron beam and filter out unwanted scattered electrons before image formation. The electron beam hits the sample and three interactions occur. Unscattered electrons represent (transmitted beam). Second are elastically scattered electrons (diffracted beam) and inelastically scattered electrons. Then, the transmitted electron is focused by an objective lens and sent to a projector

lens to expand onto a phosphor screen. Electrons strike the phosphor screen and generate light, displaying an image. Figure 2.6 represent schematic of TEM (Heinlaan et al. 2008).

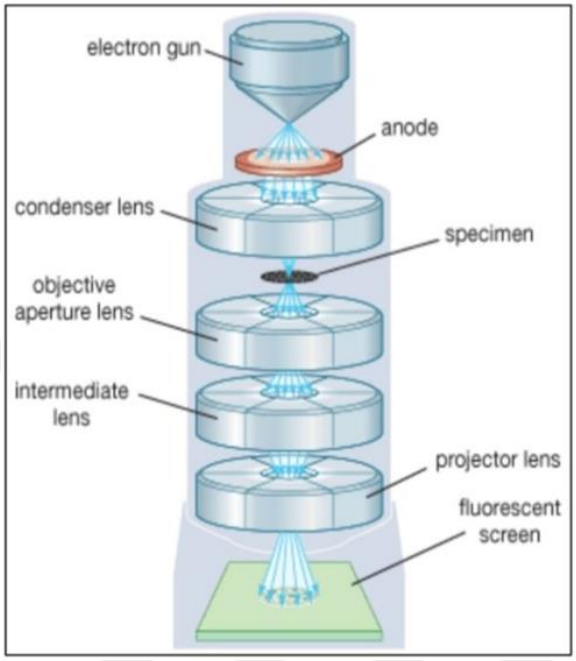

Figure 2.6 Schematic of TEM (Doyle 2006)

2.3.7 FTIR spectroscopy

FTIR spectroscopy examines amino acid and cofactor vibrational properties, which are sensitive to structural changes. Nonlinear molecules have N atoms and 3N-6 vibrational motions of molecule atoms. On the other hand, asymmetric vibrations for all molecules are detected in the midmost-infrared region (4000 - 1000) cm^{-1}. The main type of vibrations observed is stretching vibrations, which change bond-length. Figure shows a harmonic oscillator model of stretching vibrations (Figure 2.7). The molecular bond strength is spring tension (K) and atom mass (m_1, and m_2) The frequency is given by Equation (2.6).

$$\upsilon = (1/2\pi c)\sqrt{k(m1 + m2)/m1m2} \qquad (2.6)$$

Where (υ) is vibration frequency depends on bond strength $(cm)^{-1}$

(k) is spring tension

(m_1, and m_2) atom mass involved in the vibration (g)

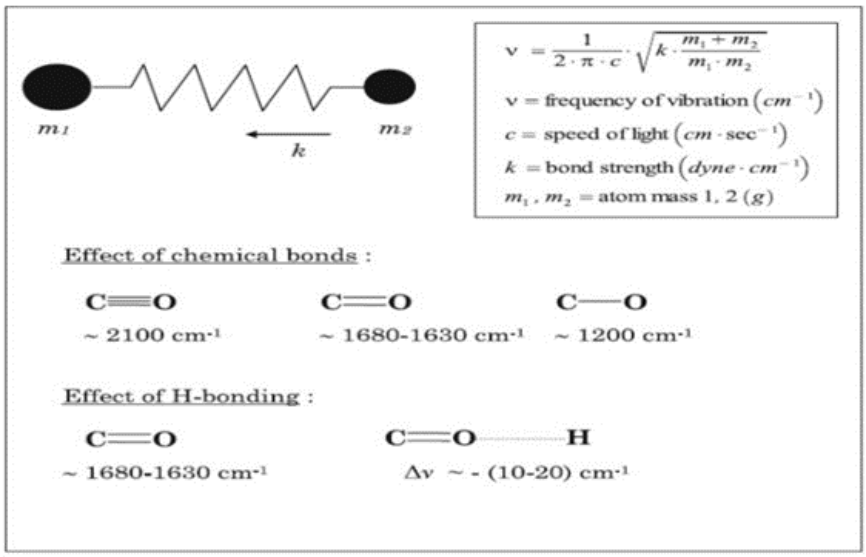

Figure 2.7 Two types of Stretching vibrations bonds (Khan *et al.* 2019)

2.3.8 XRD analysis

This is because a particle-crystalline powder specimen is usually made up of particles. In XRD analysis, "crystal size" refers to the "size of crystallites" with a factor in mind. which rise in diffraction peak is widening. when the size of a crystallised particle in a powder is less than five nanometers. If the size of the crystallites is less than 100 nm, for example, the measured XRD shows peak broadening. Figure 2.8 shows the difference between the size of a crystallite and the size of a particle.

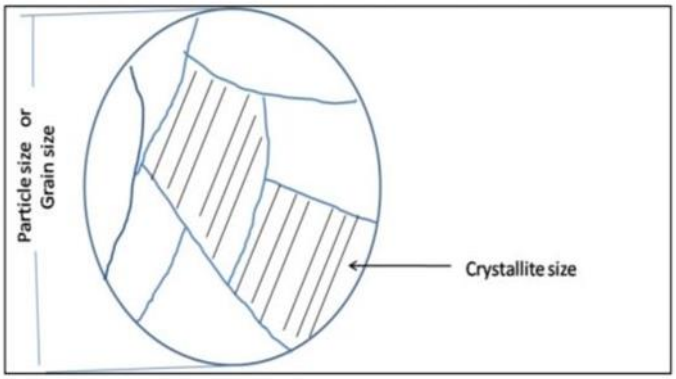

Figure 2.8 Difference between crystallite size and particle size (Waseda *et al.* 2011)

2.3.9 Photoluminescence

From the experiments, we can figure out a lot about the electronic structure of the semiconductor (Brayner *et al.* 2006). A PL study can tell you about the size of the band gap, the level of impurities, the interface and surface properties, and the number of states and exocitonic states. A PL spectrum is made by collecting the luminescence that is given off and recording the intensity as a function of the energy of the photons that are given off. In a PL measurement, the energy used to excite the sample stays the same, while the energy used to measure the sample is scanned. Radiative recombination is defined by the energy of the photon that is emitted.

The PL technique is useful for analysing discrete defect and impurity states. External forces, such as mechanical pressure, can also be used in PL investigations (Özgür *et al.* 2005, Chinnapaiyan *et al.* 2022, Ferblantier 2005). Since PL relies on radiative recombination, nonradiative processes need indirect methods, and poor-quality materials are hard to characterise with PL (Thevenot *et al.* 1999).

Surface acoustic wave devices, piezoelectric transducers, optical waveguides, acousto-optic media, transparent conductive electrodes, solar cell windows, and varistors can all be made with ZnO thin films (William 2006, Özgür *et al.* 2005, Chinnapaiyan *et al.* 2022, Ferblantier 2005).

2.4. Preparing Nano-Particles

There are different ways to make nanoparticles, which can be put into two groups: bottom-up and top-down. Bottom-up methods involve breaking down materials to their atomic level and then letting them self-assemble into nanoparticles. During self-assembly, on the other hand, basic units are linked together by physical forces that work at the nanoscale level. The most widely used methods in this approach are pyrolysis, biosynthesis, sole gel, spinning, and chemical vapour deposition (Bodnar *et al.* 2005). Both of these methods are contradictory and can be shown with a diagram in Figure 2.9.

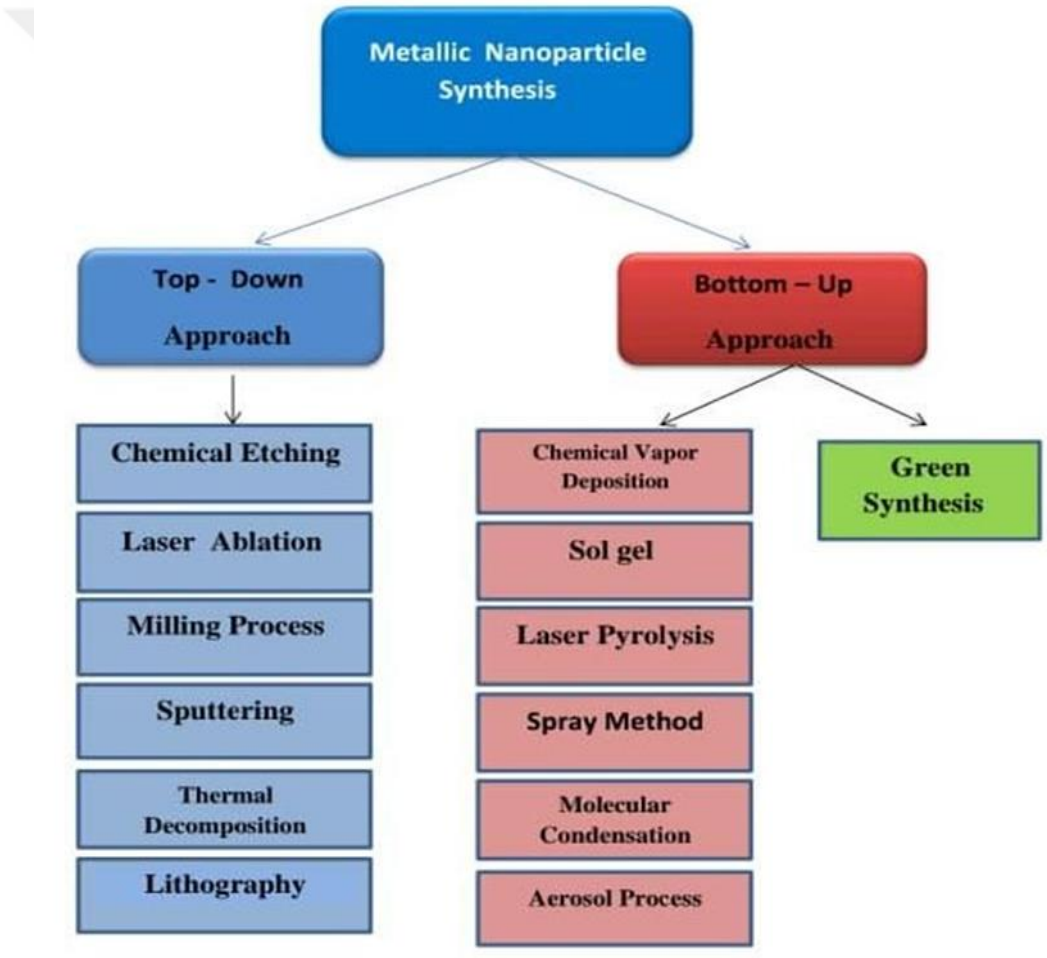

Figure 2.9 Bottom-up and top-down design methodologies are represented schematicall.

2.5 Bottom-Up Method

2.5.1 Sol-gel

Sol is a colloid in which groups of small particles are spread out in a liquid phase. They are bigger than nano-particles, which range from 1 nm to 1 m. Gels, on the other hand, are made of solid macromolecules that are dissolved in a solvent. Sol gel is one of the easiest and most frequently used ways to make nanoparticles. It is a chemical method that uses a solution as a starting point for a system of different particles. As starting materials, this method usually uses metal oxides, metal chlorides, and alkoxysilanes (usually tetramethoxy and ethoxysilanes). The sample is then dried to get rid of any moisture. The main benefits of this process are that it can make nanostructures that are uniform and pure, even at very low temperatures (Bodnar *et al.* 2005, Ramesh *et al.* 2016, Mann *et al.* 1997, Lee *et al.* 1997). This process is not easy to scale up because it has different drying steps and it is hard to control synthesis while it is happening. The sol-gel process has a lot of benefits because it is simple, it is easy to control the composition of the film, it is safe, and the equipment and raw materials are cheap. In fact, ZnO films made from sol-gel could be useful for making low-cost optoelectronic devices (Park *et al.* 2002).

It has already been seen that the thickness of a sol-gel ZnO film has a big effect on its optoelectronic properties (Mashaghi *et al.* 2013). In particular, the photoconduction properties of a polycrystalline film are controlled by the micropores at the grain boundaries, which depend on the thickness of the film (Mashaghi *et al.* 2013).

The number of coatings and the concentration of the sol can change the thickness of a sol-gel film. The viscosity of the moving liquid drags on the substrate, which affects the thickness. In this paper, we looked at the effect of sol concentration on the structural, optical, and optoelectronic properties of ZnO films grown on glass substrates using a sol–gel drain coating technique. As the concentration goes from 0.03 to 0.1 M, the structural and optical properties get better, but the UV light sensitivity is highest for a film deposited with a 0.05 M sol.

2.5.2 Chemical vapor deposition (CVD)

This approach coats the substrate with a gaseous reactant layer. A reaction chamber mixes gas molecules at ambient temperature to deposit This thin film can be recycled. This approach relies on substrate temperature. This approach produces pure, homogenous, robust, and mechanically stable nanoparticles. CVD requires sophisticated equipment, and the gaseous byproducts are hazardous (Sharma *et al.* 2020, Brayner *et al.* 2006, Lee *et al.* 1997).

2.5.6 Biosynthesis

Instead of chemicals, bacteria, fungi, and plant extracts are employed as precursors for bio-reduction and capping. Medical applications use this method's unique and enhanced features (Khan *et al.* 2018, Ahmadian *et al.* 2018).

2.5.7 Pyrolysis

Industrial pyrolysis produces nan-particles. A furnace burns precursor. The furnace burns precursor through a small aperture (Taniguchi 1994). Byproduct gases accumulate nanoparticles. Pyrolysis prepares nanoparticles well due to its simplicity, high product yield, and sensitivity (Danial *et al.* 2020, Jiang *et al.* 2016).

2.6 Top Down Techniques

2.6.1 Mechanical milling

Mechanical milling is a popular top-down nanoparticle production method. Under an inert atmosphere, different elements are milled and post-annealed (Patra *et al.* 2018, Chua 2008, Mashaghi *et al.* 2013).

2.6.2 Nano-lithography

The study of creating nanoscale "structures" with at least one dimension and dimensions between 1 and 100 nm is known as nanolithography. Lithography, which specifically evacuates a little amount of material to create the desired shape and structure, is often the method for printing a needed shape or structure onto a light-sensitive substance. The main benefit of nanolithography is the ability to produce a group of nanoparticles with the required form and size from a single nanoparticle (Stoimenov *et al.* 2002, Waseda *et al.* 2011, Husain *et al.* 2022). This procedure is efficient and requires advanced equipment.

2.6.3 Laser-ablation

Nanoparticles from solution solvents are often prepared via laser-ablation. Laser beams irradiate metals in liquid solutions, forming plasma crests that generate nanoparticles. Laser ablation synthesises nanoparticles in natural solvents and water without balancing agents or synthetics. Green process (Sharma *et al.* 2020, Amendola *et al.* 2009, Kahru *et al.* 2005).

2.7.4 Thermal decomposition

Heat breaks the compound's chemical bonds. Nanoparticles are created by rotting metal at the temperature of decomposition in an endothermic chemical process. This approach prepares metal oxide and carbon nanoparticles (Sheeparamatti *et al.* 2007, El-Kattan *et al.* 2022).

2.8 Biosensore

When electronics are applied to the fields of life and medicine, we get bioelectronics. A biosensor is a specialised bioelectronic device employed in the field of bioanalysis. An analogue or digital sensor is the "main element of a measurement chain, which turns the input variable into a signal appropriate for measurement." Several major developments in technology during the past decade have made available the resources necessary to

develop biosensor devices. To put it simply, a biosensor is a small analytical device having a biological or biologically derived sensing element that is either built into or closely linked to a physicochemical transducer.

The terms "biological recognition" and "sensing" describe two of a biosensor's primary functions. A biosensor detects molecular recognition and transforms it using a transducer. The recognition system gives the sensor exceptional analyte selectivity. The analyte-bioreceptor interaction has a measurable effect.

Information is converted into an electrical or optical signal using a transducer. A biosensor is a separately integrated receptor transducer device that makes use of a biological recognition element, in accordance with IUPAC principles. (Thevenot *et al.* 1999). Biosensors give quick, real-time, accurate, and reliable analyte information. Ideal devices respond constantly, are reversible, and don't disturb the sample. Biosensors could be used in medicine, agriculture, food safety, bioprocessing, environmental monitoring, and industrial monitoring (Long *et al.* 2006).

2.8.1 Basic principle of a biosensor

The transducer converts the biological response of the bio element to an electrical signal after it interacts with the analyte. Every biosensor has an electronic component that detects and transmits the signal and a biological component that acts as the sensor. Thus, immobilised biological material contacts the transducer. The electronic response is measured when the analyte binds to biological material to form a bound analyte. Sometimes the analyte is converted to a product that releases heat, oxygen, electrons, or hydrogen ions. A metabolic sensor measures substrate concentration by chemically changing the bioelement and analyte. The sensor is a catalytic sensor if the biological element combines with analyte and converts it to an auxiliary substrate (Figure 2.10) (Kahru *et al.* 2005).

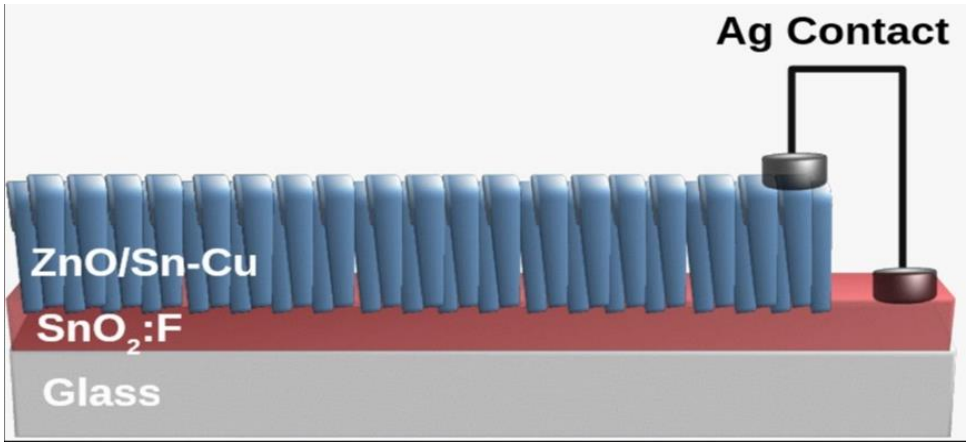

Figure 2.10 Showing the biosensor

2.8.2 Components of a Biosensor

The main parts of a biosensor are a bioreceptor, a transducer, and a signal processing system (Doyle 2006) (Figure 2.11). Biosensors can be put into groups based on their bioreceptors or transducers. Biosensors are divided into groups based on bioreceptors and transducers (Figure 2.12).

A bioreceptor is a type of molecule that can recognise something using a biochemical mechanism. They are in charge of binding the analyte of interest to the surface of the sensor so that it can be measured. In general, bioreceptors can be put into five main groups: enzymes, antibodies and antigens, nucleic acids and DNA, cellular structures and cells, and biomimicry. In biosensing, the most common;

1. Antibodyeantigen interactions

2. Nucleic acid interactions

3. Enzymatic interactions

4. Cellular interactions (i.e., microorganisms)

5. Interactions using biomimetic materials (i.e., synthetic bioreceptors) types of bioreceptors are based on:

The enzymes and antibodies are the main classes of bioreceptors that are widely used in biosensor applications.

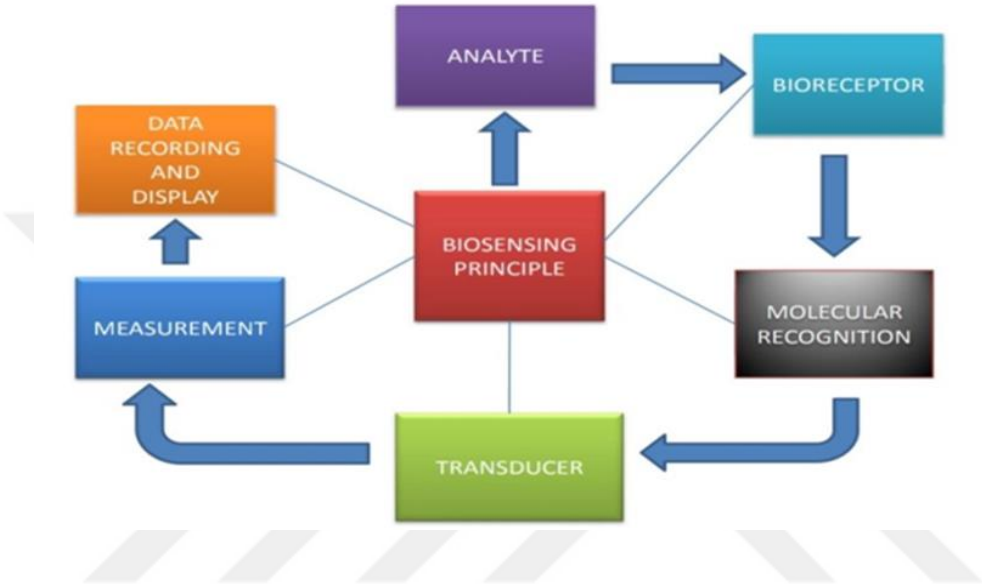

Figure 2.11 The basic idea behind biosensors

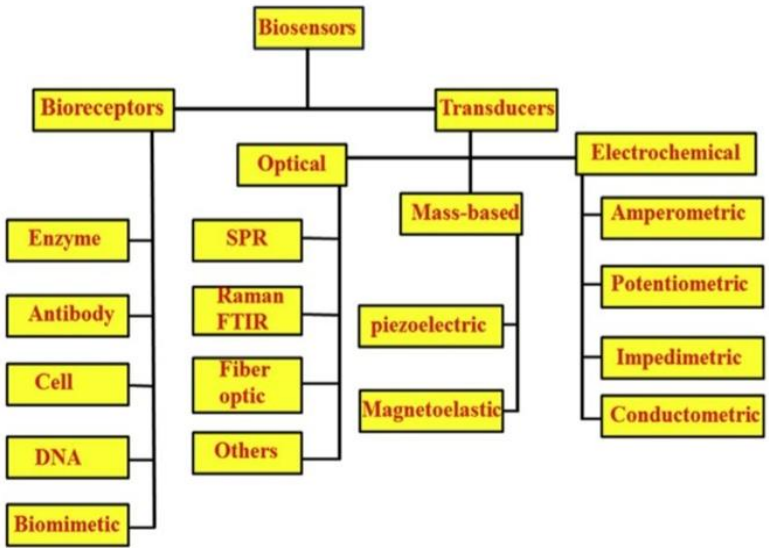

Figure 2.12 Classification of bioreceptors and transducers

2.8.3 Biosensors are enzyme receptors

In biosensor applications, enzymes have been the most common bioreceptor molecules. Enzymes are often used as bioreceptors because they can bind to specific molecules and also break down other molecules. In biocatalytic recognition mechanisms, a catalytic reaction makes the detection stronger.

Some enzymes can work without any other chemical groups besides the amino acid residues they are made of. Others need an extra part called a cofactor, which can be one or more inorganic ions like Fe^{2+}, Mg^{2+}, Mn^{2+}, or Zn^{2+}, or a coenzyme, which is a more complicated organic or organometallic molecule. Enzymes have a catalytic effect that makes it possible for detection limits to be much lower than they would be with binding techniques.

As would be predicted, the stability of an enzyme's original protein structure is a prerequisite for its catalytic activity. An enzyme's catalytic activity is lost if it is denatured, divided into its constituent parts, or broken down into its amino acids. The recognition methods can also be changed by using enzyme-coupled receptors. For instance, when a ligand attaches to a receptor, the activity of an enzyme may be altered.

An enzyme cascade frequently considerably improves this enzymatic activity and causes intricate cell responses. Like a key fitting a lock, the enzyme can identify a certain target analyte. When compared to chemical reactions, enzymes are far more sensitive and selective. They also respond rather quickly when compared to other biological receptors and can be combined with a variety of transduction processes. These bioreceptors work by one of three different mechanisms: (1) converting the analyte into a product that can be detected by the sensor; (2) detecting an analyte that acts as an enzyme inhibitor or activator; or (3) determining how the properties of the enzyme change when it interacts with the analyte.

2.8.4 Bioreceptor for antibodies: immunosensors

To find a specific antigen, an immunosensor uses antibodies as bioreceptors. Immunoassays are the most accurate way to analyse data, but they have a very low detection limit.

It has no limits and can be used for many different substances. The ability to identify and measure proteins is greatly aided by these tests (Waseda *et al.* 2011, Goncharova *et al.* 2018). Figure 2.13 shows a diagram of the Y-shaped structure of an antibody.

Antibodies, also called immunoglobins, are heavy globular proteins in the blood. They are also called glycoproteins, and they have the familiar Y shape made of two heavy chains and two light chains (Figure 2.13). They are made by animals when their immune systems react to antigens, which are foreign substances. The antibody binds to the target antigen strongly, so it can find the analyte even when there are other substances in the way. There are two types of antibodies used in the development of immunosensors: polyclonal and monoclonal. Polyclonal antibodies are very sensitive, but they are not as specific as monoclonal antibodies because they can recognise different epitopes (a small area on an antigen to which a complementary antibody can bind) on their target antigens. They also stain the background much less than polyclonal antibodies.

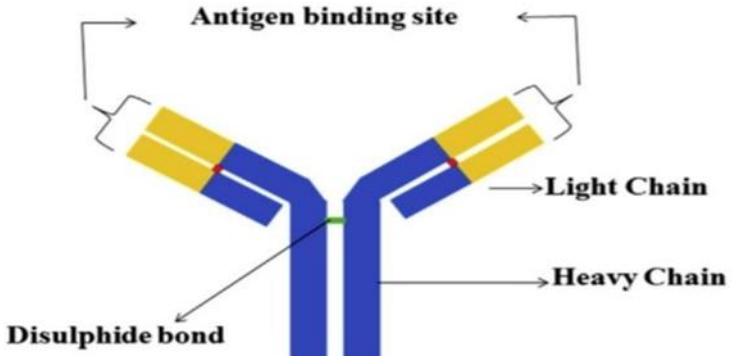

Figure 2.13 A schematic of an antibody's Y-shaped structure

2.9 Antimicrobial activity of nanoparticles of zinc oxide

Zinc oxide nanoparticles are well-known for their antibacterial properties and their ability to prevent microbial development by penetrating cell membranes. Lipids, carbohydrates, proteins, and DNA are all harmed by the oxidative stress (Kelly *et al.* 1998). Without a doubt, lipid peroxidation is the most important cause of cell membrane modification, which in turn disrupts essential cellular activities (Rikans and Hornbrook 1997). The use of zinc oxide nanoparticles in an oxidative stress mechanism in Escherichia coli lends credence to this theory (Zhang *et al.* 2007).

External creation of H_2O_2 has been proposed to characterise the antibacterial characteristics for bulk zinc oxide solution. Another factor taken into account is the potential danger posed by nanoparticles due to the harmful ions they release. Zinc oxide is amphoteric, therefore it releases Zn^{+2} ions when exposed to acids and alkalis, as given in Equation (2.7), Equation (2.8), and Equation (2.9).

$$ZnO + 2HCl \rightarrow ZnCl_2 + H_2O \quad (2.7)$$

$$ZnO + 2NaOH \rightarrow Na_2ZnO_2 + H_2O \quad (2.8)$$

$$ZnCl_2 \rightarrow Zn^{+2} + 2Cl^- \quad (2.9)$$

When free Zn^{+2} ions interact with biomolecules like proteins and carbohydrates, the bacteria are rendered incapable of carrying out their normal tasks. However, metal oxide nanoparticles do not need to penetrate the bacterial cell to be poisonous (Heinlaan *et al.* 2008). The mere contact of nanoparticles with the cell wall is enough to produce toxicity. If this is right, then vast numbers of metal nanoparticles are necessary to totally wrap and insulate the bacterial cells from their environment, leaving no possibility for nourishment to be absorbed to continue the life process. Because nanoparticles and metal ions are smaller than bacterial cells, they are more likely to break the cell membrane and limit growth (Hussain 2008). Externally, zinc oxide nanoparticles are used to treat moderate bacterial infections, but the zinc ion is an important trace element

for some viruses and humans, increasing the enzymatic activity of viral integrase (Brayner *et al.* 2006, Elster *et al.* 1994).

It has also been shown that when treated with 10 mg/L of Zn, the infectious pancreatic necrosis virus increases by 69 % (Husain *et al.* 2007). It might be because Zn ions are more soluble than ZnO alone. Zinc oxide nanoparticles have been demonstrated in SEM and TEM figures to disrupt the bacterial cell wall (Zhang *et al.* 2007, Adams *et al.* 2006) and enhance permeability, followed by their accumulation in *E. coli*, impeding growth (Brayner *et al.* 2006).

Staphylococcus aureus, *E. coli*, *Salmonella typhimurium*, and *Klebsiella pneumoniae* are four well-known gram-positive and gram-negative bacteria. Recently, the antibacterial activity of zinc oxide nanoparticles against these four bacteria has been investigated. The growth inhibitory dosage of zinc oxide nanoparticles was found to be 15 g/ml, while it was as low as 5 g/ml in the case of *K. pneumoniae* (Brayner *et al.* 2006, Stoimenov *et al.* 2002).

It has been discovered that as the concentration of nanoparticles grows, so does the suppression of microbial development. Growth was substantially suppressed when they were incubated for 4-5 hours with a maximum concentration of zinc oxide nanoparticles of 45 g/mL. It is hypothesised that increasing the incubation period would boost growth inhibition without affecting the mechanism of action (Brayner *et al*. 2006).

Researchers have shown that metal oxide nanoparticles may penetrate the membrane of bacteria and cause harm before entering the cell (Stoimenov *et al.* 2002). Additionally, H_2O_2 emission has been suggested as a potential replacement for antibacterial action. However, this hypothesis has to be tested in the lab to be accepted, as zinc oxide nanoparticle presence alone is insufficient to generate hydrogen peroxide. Nanoparticles of zinc or zinc oxide at such a low concentration that they cannot be detected by the human senses are not hazardous. Zinc is a mineral that must be consumed on a daily basis in order to maintain normal metabolic processes. It is well established that zinc oxide prevents *E. coli* from damaging the digestive system and stomach (Yang *et al.*

2021). Zinc oxide in the stomach can react with acid to form Zn^{2+} ions since the stomach's pH ranges from 2 to 5.

The toxicity of zinc oxide nanoparticles against both prokaryotic and eukaryotic cells has been observed by Premanathan *et al.* (2011). Zinc oxide nanoparticles were shown to have a MIC of 500 and 125 g/ml against Escherichia coli, Pseudomonas aeruginosa, and Staphylococcus aureus, respectively (Premanathan *et al.* 2011). The toxicity of zinc oxide nanoparticles has been attributed to two different mechanisms: (1) the production of reactive oxygen species (ROS) and (2) the triggering of apoptosis. Cells exposed to metal oxide nanoparticles experience oxidative stress, which leads to increased reactive oxygen species (ROS) generation and therefore, damage to cellular components such lipids, proteins, and DNA (Long *et al.* 2006). Therefore, zinc oxide nanoparticles cause toxicity via apoptosis. Although they are nonselective, they are considerably more harmful to cancer cells than normal cells.

Zinc oxide nanoparticles have been demonstrated recently by Pati *et al*. (2014) to compromise the membrane integrity of bacteria, decrease the hydrophobicity of cell surfaces, and inhibit the transcription of genes involved in bacterial resistance to oxidative stress (Pati *et al.* 2014). By stimulating the generation of reactive oxygen species (ROS), they improve intracellular bacterial death. These nanoparticles prevent pathogen-made hemolysin toxin from disrupting biofilm development and causing hemolysis. Zinc oxide nanoparticles, when injected intradermally, significantly reduced skin infection and inflammation in mice and enhanced the structural integrity of affected skin. Researchers have shown that metal oxide nanoparticles may penetrate the membrane of bacteria and cause harm before entering the cell (Stoimenov *et al.* 2002) . In addition, it has been suggested that H_2O_2 emission might have antibacterial effects (Yamamoto *et al.* 2004). Since the presence of a zinc oxide nanoparticle alone is insufficient to generate hydrogen peroxide, confirming this hypothesis would need experimental work. Ultra-low concentrations of zinc or zinc oxide nanoparticles are not harmful to human cells. In order to maintain normal metabolic processes, zinc must be consumed daily through meals. Zinc oxide has been shown to prevent *E. coli* from damaging the digestive system and stomach (Yang *et al.* 2021).

3. MATERIAL AND METHOD

In this study, metal samples, which were integrated into the FTO surface (undoped, ZnO/Sn-Cu %1, ZnO/Sn-Cu %2, and ZnO/Sn-Cu %3) samples were used.

3.1. SILAR Method

In 1985, Y. Nicolau's report on ZnS and CdS deposition introduced the protocol for SILAR deposition of thin films. In the same year, Ristov et al. used this technique to deposit polycrystalline copper oxide (Cu_2O) (Nicolau 1985, Ristov *et al.* 1985).

Nicolaus came up with a method that uses aqueous solutions of $CdSO_4$ or $ZnSO_4$ as a source of metal and Na_2S as a source of sulfur. Everything is kept at room temperature. The substrate was then put into each solution, with steps of rinsing in between to get rid of any extra precursor. The temperature of the 2 m NaOH solution was kept between 60 and 80 °C, while the temperature of the $Cu_2S_2O_3/Na_2S_2O_3$ complex solution was kept at room temperature.

Because the films made in these two studies had good structural, optical, and electronic properties, the technique was used to make more films. In the same decade, the technique was used to deposit a wide range of metal chalcogenides (Patra *et al.* 2018, Nicolau 1985).

As of now, scientists are very interested in SILAR, and it has been proven to be an easy way to deposit thin films of oxides, peroxides, hydroxides, sulphides, selenides, and more complex heterostructured systems on a desired substrate (Mann *et al.* 1997, Ahmadian *et al.* 2018).

Based on what has been said about SILAR and how it compares to other popular coating techniques, the following are some of the unique features and benefits of this method. Most of the time, the thin film is put on a rigid, flat surface with no size restrictions. The thickness of the films can be easily adjusted. By controlling the

concentration of species and the number of deposition cycles, the thickness can be made to vary over a wide range (from about one atomic layer to a few microns). SILAR depositions are usually done at room temperature, which makes them easy to do, saves energy, and doesn't limit the materials that can be used for the substrate.

Plastics, which are sensitive to temperature, can be used to deposit films, and the corrosion or oxidation of metal support substrates can be lessened by choosing the right precursors. If needed, coatings that have already been deposited can be annealed after deposition to promote crystallisation, grain growth, etc. Also, because ionic reactions at the interface between the solution and the substrate can be controlled, the deposited films can be made to have a certain crystallographic orientation and grain structure.

The SILAR method also makes it more likely that a film will only grow on the part of the substrate that is in contact with the solution. This keeps reactants from being wasted unnecessarily (Thevenot *et al.* 1999, Pati *et al.* 2014, Mashaghi *et al.* 2013).

If needed, precursor solutions could also be reused and refilled, as long as they don't change over time. So, SILAR is a very powerful and flexible method for depositing many thin-film materials that are of great interest to technology. In the sections that follow, we'll talk about the theory behind SILAR deposition and then look at how metal oxides can be made using this method, focusing on how the deposition parameters affect the properties of the films that are made. We'll end the review by looking at some of the most promising uses of oxides made with SILAR and giving an overview of what else needs to be done in this field.

3.2 Effect of SILAR Process Experiment Parameters

As we've already demonstrated, the SILAR process' experimental settings have an impact on the materials' quality and functionality. The shape, structure, and function of the coating that is deposited can all be affected by temperature, ion concentration, residence duration, pH of the solutions, and the presence of surfactants and complexing agents. For example, they can change how reactive the species are as a whole and how

fast the film forms (Ahmadian *et al.* 2018, Kahru *et al.* 2005). It has also been shown that the surface treatment or functionalization of the substrate before the SILAR process can change the quality of the films that are deposited.

3.3 For The Purpose of Preparing the Solution

The fundamental material for the samples to be created was glass that had been coated with SO_2. SnO_2:F-coated glassware, type TEC8, dimensions 25 mm x 25 mm, and thickness 2 mm The SnO_2:F-coated glasses were thoroughly cleaned before magnification. The SnO_2:F-coated coated glasses were washed in soapy water to remove any dirt that had formed on them as the first stage in the cleaning procedure. After being rinsed, glass substrates coated with SnO_2:F-coated were ultrasonically cleaned in acetone for ten minutes. After that, it was given a ten-minute ultrasonic treatment in a solution consisting of equal parts water and ethanol (1:1). (Figure 3.1).

Figure 3.1 Solution that have been prepare in lab

3.3.1 ZnO thin films were grown on a SnO_2:F/Glass substrate

The zinc-ammonia complex $[Zn(NH_3)^4]^{2+}$ was applied to the SnO_2:F/Glass substrate to facilitate the formation of ZnO thin films. The Zinc-Ammonia solution complex was made by mixing 0.1 M $ZnCl_2$ (pH 5.5) solutions with 25-28 % NH_3 solutions in a 1:10 molar ratio. This made it possible for the zinc-ammonia solution complex to be made.

Here's a list of the chemical reactions that happen during the growth phase of thin films: as given in Equation (3.1), Equation (3.2), Equation (3.3), and Equation (3.4).

$$ZnCl_2 + 2NH_4OH \leftrightarrow Zn(OH)_2 + 2NH_4^+ + 2Cl^- \quad (3.1)$$

$$Zn(OH)_2 + 4NH_4^+ \leftrightarrow [Zn(NH_3)_4]^{2+} + 2H_2O + 2H^+ \quad (3.2)$$

$$[Zn(NH_3)_4]^{2+} + 4H_2O \rightarrow Zn(OH)_2\,(s) + 4NH_4^+ + 2OH^- \quad (3.3)$$

$$Zn(OH)_2\,(s) \rightarrow ZnO(s) + H_2O \quad (3.4)$$

Figure 3.2 Experiment to deposit ZnO thin sheets by SILAR method

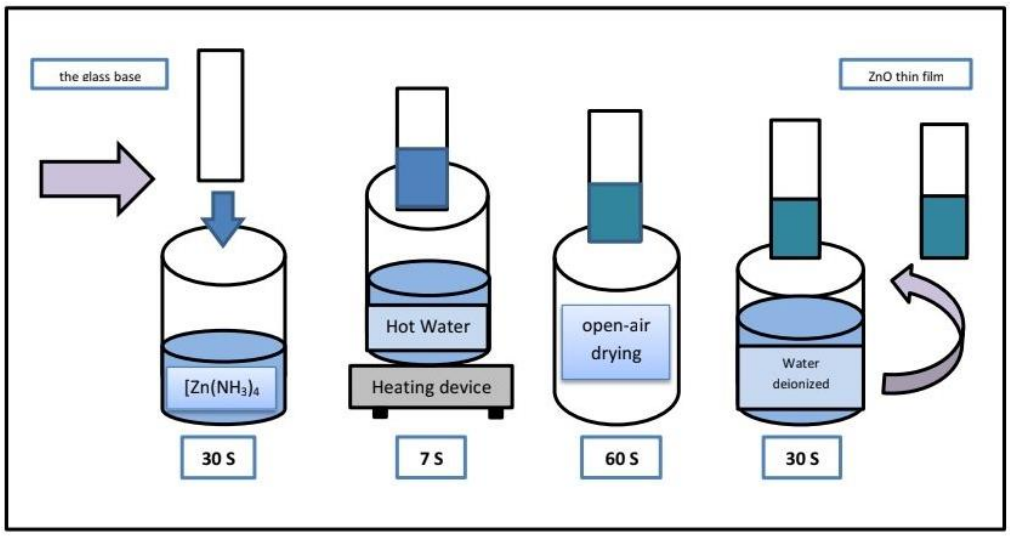

Figure 3.3 Schematic of an experiment to deposit ZnO thin sheets by SILAR method

In order to create ZnO thin films, it is necessary to follow a four-step process, the first of which is solution preparation. A SILAR cycle is complete after each of these four processes has been completed. The first step is to soak the substrate for 30 seconds in a solution of $[Zn(NH_3)^4]^{2+}$. The second step is to remove the substrate from the solution and let it sit in boiling water at 90 degrees Celsius for seven seconds. The third step is a sixty-second period of air drying the substrate. When the surface is washed for 30 seconds in sterile water, the final phase of the SILAR process, large ZnO particles with weak connections are washed away. This process will be repeated until the entire area has been coated evenly. In Figure 3.2, we see a simplified illustration of the SILAR method for fabricating ZnO thin films. Forty iterations of such deposition cycles were performed (Figure 3.3).

3.3.2 The growth of Sn-Cu doped ZnO thin films on SnO_2:F/Glass substrate

To produce Sn-Cu-doped ZnO samples, a SnO_2:F/Glass substrate was created, and subsequently, the SnO_2:F/Glass substrate was cleaned. After cleaning, solutions containing the appropriate additives were prepared, and Sn-Cu doped ZnO thin films were produced on SnO_2:F/Glass using the SILAR technique. Here are some of the

chemical changes that occur throughout the development phase, as given in Equation (3.5), Equation (3.6), Equation (3.7), and Equation (3.8).

$$ZnCl_2 + 2NH_4OH \leftrightarrow Zn(OH)_2 + 2NH_4^+ + 2Cl^- \quad (3.5)$$

$$Zn(OH)_2 + 4NH_4^+ \leftrightarrow [Zn(NH_3)_4]^{2+} + 2H_2O + 2H^+ \quad (3.6)$$

$$SnCl_2 + 2NH_4OH \leftrightarrow Sn(OH)_2 + 2NH_4^+ + 2Cl^- \quad (3.7)$$

$$Sn(OH)_2 + 4NH_4^+ \leftrightarrow [Sn(NH_3)_4]^{2+} + 2H_2O + 2H^+ \quad (3.8)$$

When solutions of $ZnCl_2$, $SnCl_2$, and NH_3 are mixed, the reactions listed above happen, and a complex of $[Zn(NH_3)^4]^{+2}$and $[Sn(NH_3)^4]^{2+}$ (pH 10) is made. $[Zn(NH_3)^4]^{+2}$ $[Cu(NH_3)^4]^{2+}$ and a zinc-ammonia complex. Cn-doped ZnO thin films are made with indium-ammonia complexes. 0.1 M $ZnCl_2$ (pH 5.5), 0.1 M $CuCl_2$ (pH 5.5), and 25-28 % NH3 solutions are used to make $[Zn(NH_3)^4]^{+2}$, $[Cu(NH_3)^4]^{2+}$, and complexes.

The $[Zn(NH_3)^4]^{+2}$ and $[Cu(NH_3)^4]^{2+}$ complexes are mixed in the right amounts based on the 1 %, 2 %, and 3 % Cu doping ratios, and the Sn-Cu doped ZnO thin films are shown above. It was grown in steps on a SnO_2:F/Glass (FTO) substrate (Figure 3.4). So, Sn-Cu doped ZnO thin films with doping ratios of 1 %, 2 %, and 3 % Cu were made using the SILAR method on a base of SnO_2:F/Glass. These were called FTO/Sn-Cu doped ZnO thin films.

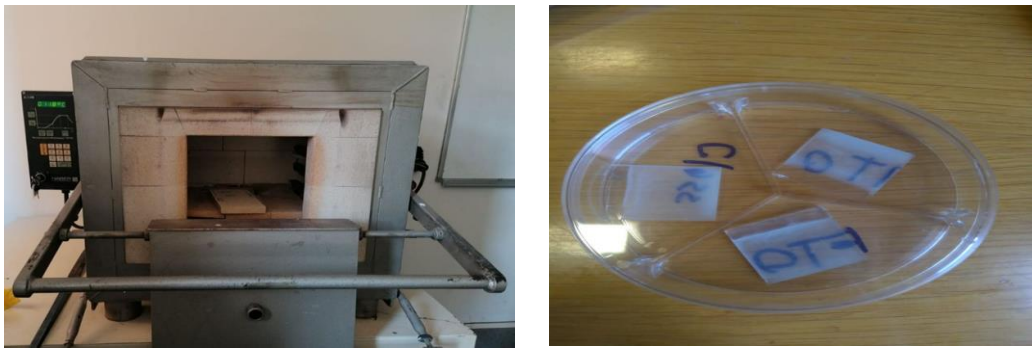

Figure 3.4 Shows the drying stage of the glass slide

3.3 Scanning Electron Microscopy (SEM)

In SEM, the material is looked at with a raster of very intense, focused electron beams. The electron beam and sample electrons could interact in different ways to make different things happen. Most of the electron beam hits the specimen and is spread out both inelastically and elastically. First, the orientation of the fundamental electrons changes, but their energy stays the same. Electrons that are not elastic scatter and lose energy. Most of the energy from the electron beam is turned into heat in the object, but there are also other effects. After that, there may be secondary electrons, electrons that bounce back, and X-rays. When an incoming electron changes direction and loses energy, it gives that energy to an atom in the sample (this is called an inelastic event) and leaves the sample with not much energy. Each electron that comes in can make many secondary electrons, which is why they are the most common signal for imaging in SEM. Backscattered electrons are made when an incoming electron hits an atom in the sample, loses energy, and scatters 180 degrees in all directions. Some of the backscattered electrons turn into secondary electrons when they leave the specimen. Backscattered electrons are made based on the atomic numbers of the chemical elements in the sample. The area gets brighter as the number of atoms goes up. X-rays are made when an atom in the sample loses some of its energy. As we'll talk about below, this signal is very important for analysis. The interaction volume is the area where the electron beam goes through the specimen, or the three-dimensional space made by the interaction of the electron beam with the atoms of the specimen. SEM emission depth depends on the energy of the electron beam, the type of specimen, its composition, and how the sample is prepared.

The volume of interaction grows as the voltage used to speed up the electron beam goes up. Secondary electrons (topography) and backscattered electrons are used in SEM imaging (atomic number). Analytical X-rays look at both the size and quality of a sample. So, SEM gives information about topography, morphology, composition, and crystallography. Some ideas are the same for both optical and electron microscopes.

SEM delivers more information and has fewer limits than optical microscopy. For compounds susceptible to electron beams, there are two alternatives to the classic SEM: the low-voltage microscope and the environmental SEM (ESEM). The former enables high-resolution imaging down to tens of volts, which is critical for charge reduction. It is necessary to use a lower voltage and a high beam current.

The ESEM is a typical SEM that can operate at pressures ranging from low to distilled water viewing pressure. This microscope can look at things that aren't coated because collisions with gas molecules spread electrical charges and electrons from the electron beam (Goncharova *et al.* 2018, Khan *et al.* 2018).

3.4 Energy Dispersive X-Ray Spectroscopy

High-energy photons called X-rays are created when an accelerated electron beam collides with a substance. An electron from the metal's K-shell is removed by the incident electron, leaving a void or hole. Each chemical element undergoes these transitions, which prompted the invention of EDS detection methods for electron microscopy and the expansion of their use to the microstructural characterization of materials. Interaction volume and X-ray generation volume are critical components in the final EDS spectrum (Figure 3.5). Signal strength relies on X-ray energy and sample atomic weight. Carbon Ka, X-rays are rapidly absorbed by solid samples and only a few are detected. Harder X-rays, like iron Ka, can break solid specimens and absorb little. Electron microscopy uses these X-rays to analyse chemicals. A specimen's X-ray spectrum gives qualitative and quantitative information on its elements and their amounts. Since the interaction volume varies on the incident beam diameter and beam dispersion generated by elastic scattering, microanalysis spatial resolution depends on the specimen. Increasing spatial resolution reduces a chemical element's detection limit. Higher spatial resolution reduces examined volume and signal intensity (Goncharova et al. 2018).

Figure 3.5 Energy dispersive X-ray spectroscopy

3.5 Determination of Antimicrobial Activity

Antimicrobial activities of the samples were determined by two different methods. Firstly, antimicrobial activities of the powder samples against Gram-nagative (Escherichia coli ATCC 35218) and Gram-positive (Staphylococcus aureus ATCC 25923) pathogenic bacteria were determined by the agar well diffusion method (Figure 3.6) (Reygaert *et al.* 2009, Randall *et al.* 2013). Test bacteria were grown in Nutrient broth (Merck) and their density was adjusted to McFarland 0.5. 100 µL of individual test bacteria were transferred onto the Nutrient solid medium and the bacteria inoculated on the medium were homogeneously dispersed. Then, wells with a diameter of 7 mm were opened on the solid medium with a sterile swab. 100 µL of samples at different concentrations (10, 25, 50, 100, 250, 500, 1000, 1500, 2000, 3000, 4000, and 5000 µg/mL) were added to the wells drilled in separate plates and incubated at 37 °C for 24 hours. At the end of the incubation, the diameter of the zones formed around the well was measured with a calliper and the results were given in millimetres. All studies were performed in 3 repetitions.

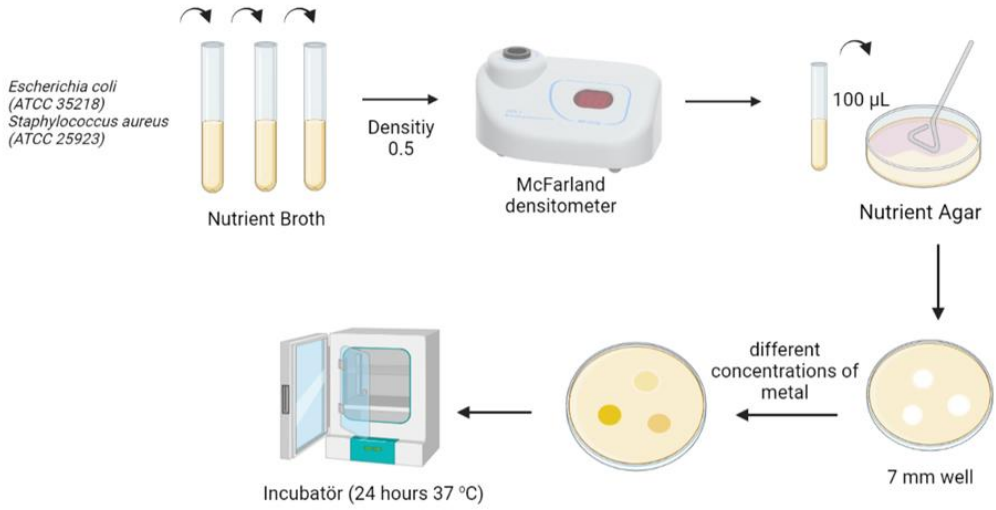

Figure 3.6 Agar well diffusion antimicrobial activity method steps

The second method is similar to the first method, the test bacteria (*E. coli ATCC 35218*, *S. aureus ATCC 25923*) density was adjusted to McFarland 0.5. Individual test bacteria were transferred (100 µL) onto the Nutrient solid medium and dispersed homogeneously. Then, different metals (undoped, ZnO/Sn-Cu %1, ZnO/Sn-Cu %2, and ZnO/Sn-Cu %3) were integrated into the glass surface, which was cut into small pieces, and placed on the test bacteria. Incubated at 37 °C for 24 hours. It was determined if there was any zone created at the end of the incubation period.

3.6 MIC and MLC/MBC Analysis

The Minimum Inhibitory Concentration (MIC) is the minimum concentration that prevents the growth of bacteria. The Minimum Lethal/Bactericidal Concentration (MLC/MBC) is defined as the minimum concentration at which no growth occurred in the medium (Al-Hada *et al.* 2018). Bacteria samples were grown in Nutrient broth and their density was adjusted to McFarland 0.5 (~1.5x108 CFU/mL). Solutions containing powder metals at different concentrations (10 - 5000 µg/mL) were prepared. 50 µL of bacteria, 50 µL of metal and 100 µL of Nutrient medium were inoculated in 96 - well plate wells and incubated at 37 °C for 24 hours. At the end of the incubation period, 10

µL was taken from the wells and dropped onto Nutrient agar. It was re-incubated at 37 ˚C for 24 hours. All studies were performed in 3 repetitions. In the study, the bacteria were used as the positive control while the metal was used as the negative control.

3.7 Survival Organism Counting Method

The lid of the Petri dish was covered with coarse blotting paper and moistened with water. The metal samples integrated into the glass surface were placed in a standard petri dish with damp filter paper on the lid. 100 µL of the bacterial solution was placed on the glass samples cut into small pieces and incubated at 37 °C for 24 hours (Vartiainen *et al.* 2005). After the incubation, the samples were taken into the tube containing phosphate-buffered saline (PBS) (0.02 % KCl, 0.144 % Na_2HPO_4, 0.8 % NaCl, 0.024 % KH_2PO_4, pH 7.0) solution to determine the number of viable bacteria on the surfaces. Vortexing was applied for 5 minutes to transfer the bacteria on the surface to the solution. After serial dilution using 0.875 % NaCl, 100 µL of bacteria was added to the Nutrient solid medium, the spreading plate method was applied and left in an oven at 37°C for 24 hours. At the end of the waiting period, the colonies that grew in the petri dishes were counted and the number of viable bacteria was calculated according to the formula below Equation (3.9), and Equation (3.10).

$$\text{Number of Viable Bacteria (CFU/mL)} = \frac{\text{(Number of colonies x Dilution factor)}}{\text{Bacteria planted in petri dish (mL)}} \quad (3.9)$$

$$\text{Dilution factor} = \frac{1}{\text{Dilution ratio}} \quad (3.10)$$

3.8 Determination of Bacterial Adhesion

Cut into small pieces, the metal samples integrated into the glass surface were placed in a sterile petri dish. On each sample, 1 mL of bacteria from the bacterial culture whose density was adjusted to McFarland 0.5 was added and kept at 37 °C for 4 hours. At the

end of the waiting period, a gentle wash with PBS was applied 3 times in order to completely remove the bacteria that did not adhere to the glass surface (Chua *et al.* 2008). Then, the samples were taken into 1-2 mL of PBS and kept in an ultrasonic bath for 2 minutes to allow the bacteria on their surfaces to pass into the solution, and then vortexed for 1 minute. This process was tried in 3 different ways, by applying sonication (2 min) instead of an ultrasonic bath and without applying any physical processes. After serial dilution using 0.875 % NaCl, 100 µL of bacteria was added to the Nutrient solid medium, the spreading plate method was applied and left in an oven at 37 °C for 24 hours. At the end of the waiting period, the colonies that grew in the Petri dishes were counted and the number of viable bacteria was calculated.

4. RESULTS AND DISCUSSION

Because of its direct and broad band gap (approximately 3.4 eV at ambient temperature), large exciton binding energy, piezoelectric characteristics, high permeability, and high electro-optical coefficients, ZnO is favoured in many technological applications. It's frequently employed in industrial applications like as gas sensors, biosensors, piezoelectric devices, and solar cell applications, both with and without ZnO doping.

Doping ZnO films with III-V group elements including Sn, Cu, Al, Ni, Ga, and In enhances their electro-optical characteristics. Structure, morphology, and optical characteristics of SILAR-grown Sn-Cu-doped ZnO films were studied.

Evaluation techniques and findings for Sn-Cu doped ZnO samples are discussed. SEM and EDX analyses on Sn-Cu doped ZnO thin films made using the SILAR process were carried out, and the findings were analysed.

4.1 Structural and Morphological Properties of Sn-Cu doped ZnO Thin Films

The Sn-Cu doped ZnO samples, the samples made in 40 cycles were annealed at 300 ^{o}C. 1%, 2%, and 3% Cu doped thin films were made with the SILAR method by keeping the 1% Sn ratio the same. The doping ratio determined how much Cu was added. The doped ZnO thin films that were made were different in structure, shape, and chemistry.

4.1.1 Energy dispersive X-ray analysis

Spectra with peaks corresponding to the elements reveal the data obtained from EDS analysis. This reveals the true composition of ZnO films. A physical technique, EDS technology provides measurements and dimensions.

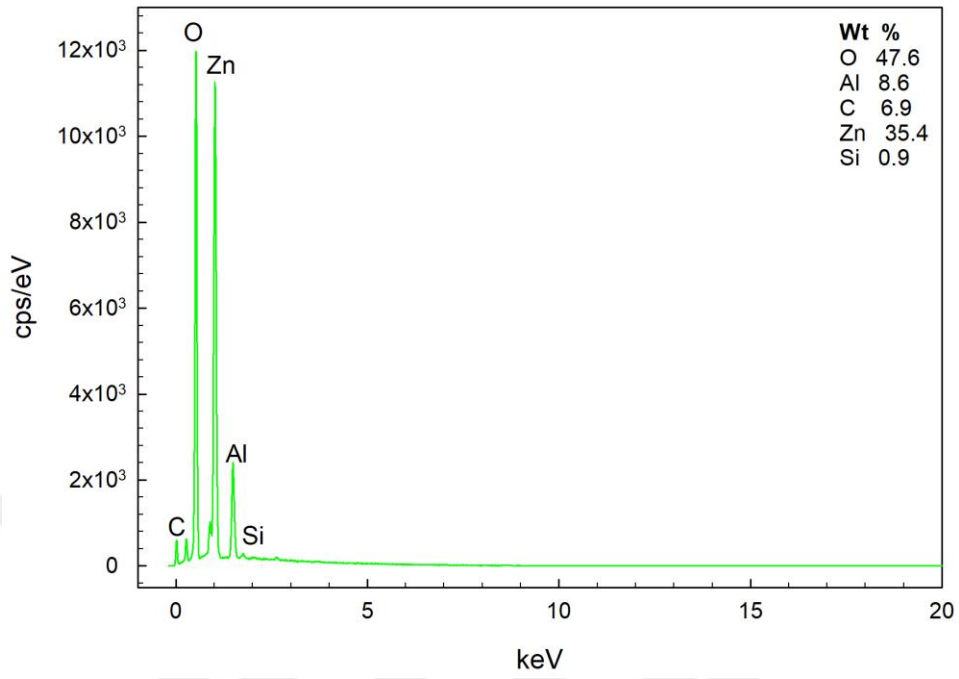

Figure 4.1 Shows the percent of FTO/ZnO, which is as follows (O 47.6 %, Al 8.6 % , C 6.9 % , Zn 5.4% , Si 0. 9 %)

Figure 4.1, Figure 4.2, Figure 4.3, and Figure 4.4 shows how the percentage of zinc changes with concentration, as shown in Table 4.1.

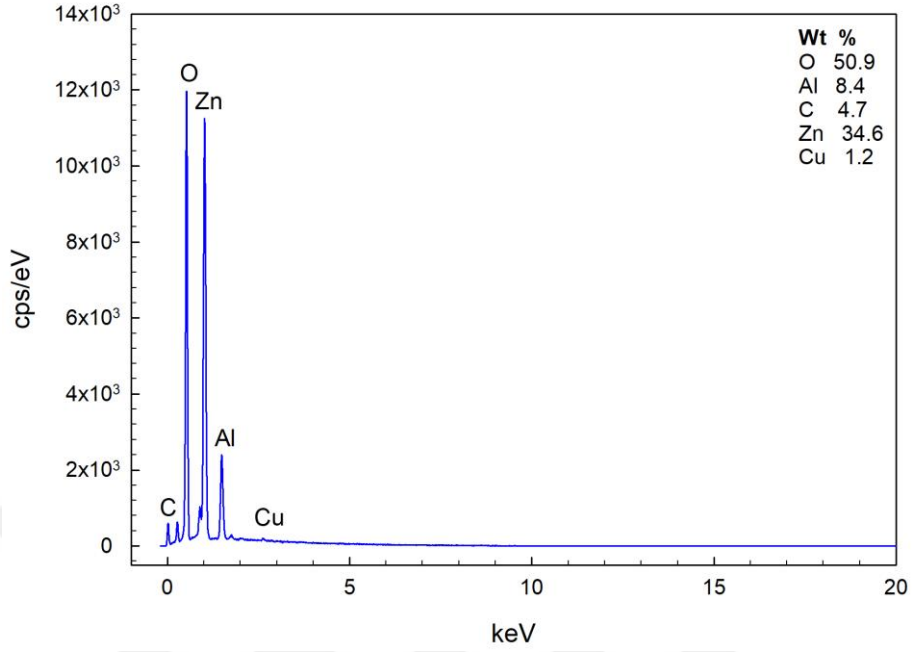

Figure 4.2 FTO/ZnO/Sn-Cu %1 EDS analysis of thin films

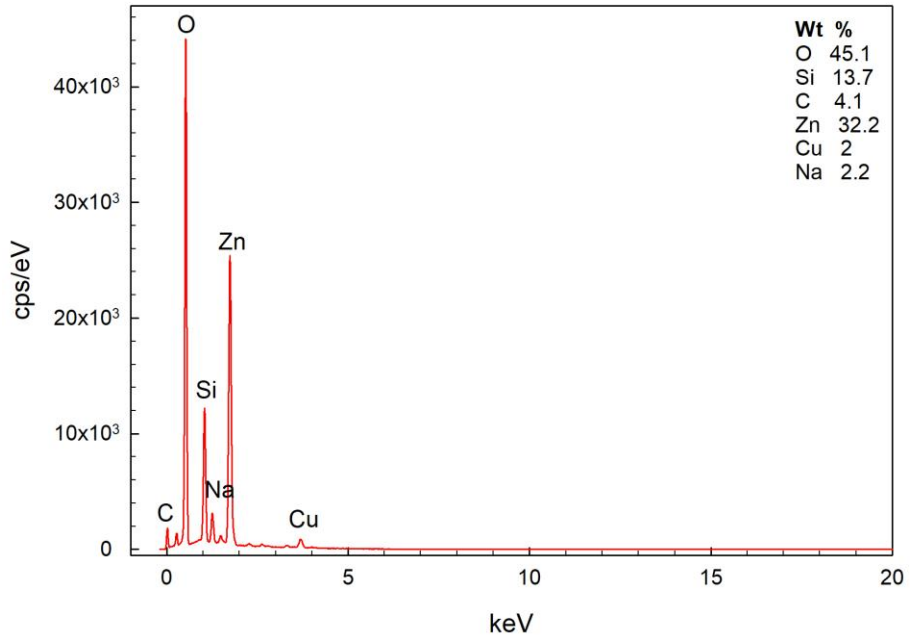

Figure 4.3 FTO/ZnO/Sn-Cu %2 EDS analysis of thin films

Figure 4.3 shows the atomic analysis of the thin flim FTO/ZnO/Sn-Cu %2, which has the following elements and vertices: (O 45.1 %, Si 13.7 %, C 4.1 %, Zn 32.2 %, Cu 2 %, Na 2.2 %).

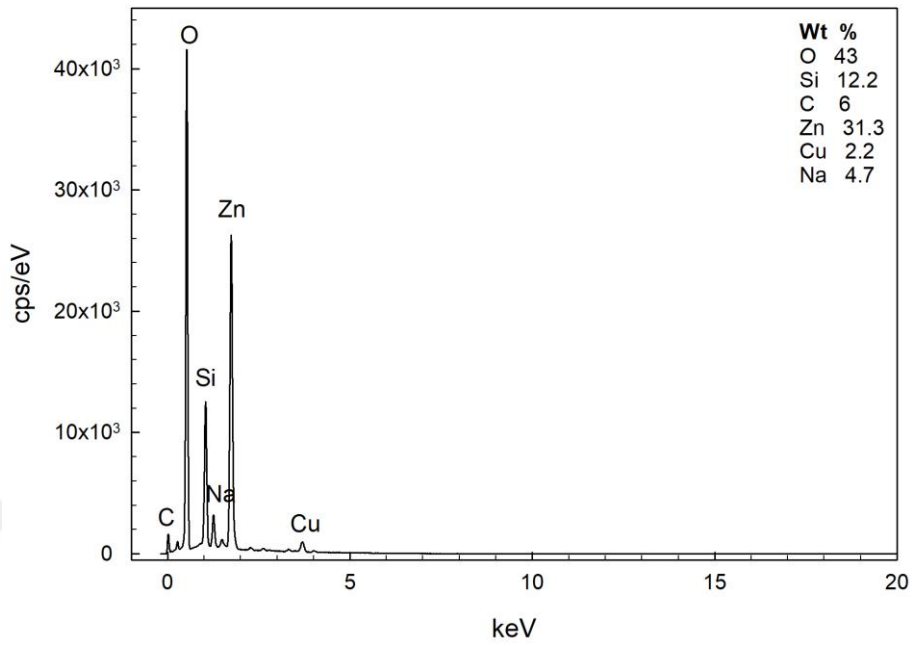

Figure 4.4 FTO/ZnO/ Sn-Cu %3 EDS analysis of thin films

Table 4.1 EDS analysis of thin films

Sample name	Zn Wt%	Si Wt%	O Wt%	C Wt%	Na Wt%	Cu Wt%	Sn Wt%	Al Wt%
FTO/ZnO	35.4	0.9	47.6	6.9	-	-	-	8.6
FTO/ZnO/ Sn-Cu %1	34.6	-	50.9	4.7	-	1.2	-	8.4
FTO/ZnO/ Sn-Cu %2	32.2	13.7	45.1	4.1	2.2	2	-	-
FTO/ZnO/ Sn-Cu %3	31.3	12.2	43	6	4.7	2.2	-	-

4.1.2 The results of a study using a scanning electron microscope (SEM)

This technique is used to characterise items with a diameter of 10 μm or less but of varying shapes and sizes.

X-ray electron microscopy and analysis of the elements By using CEM to take high-resolution figure of crystal formation and DXS, which we used as a reference method in this work with enough magnification to do a thorough analysis of the elements, we were able to look at the shape of the surface crystals. What we already thought was true was confirmed by the DXS results.

When the SEM figure of the undoped ZnO/FTO thin films were inspected, a less thick layering was developed on the FTO surface that was not homogenous with ZnO. With the addition of Sn-Cu, local condensation was seen on the FTO surface, where voids were reduced. The morphological density on the FTO surface grows as the Cu element in the solid ratio increases. The stratification on the FTO surface becomes more intense as the additive ratio increases. The roughness of the morphological structure rises. This condition raises the surface ratio, and it is predicted that the created samples will improve sensor detectability.

In general, nan crystalline structures form in tandem with the FTO surface, ZnO, and Sn-Cu doped ZnO materials as shown in Figure 4.5.

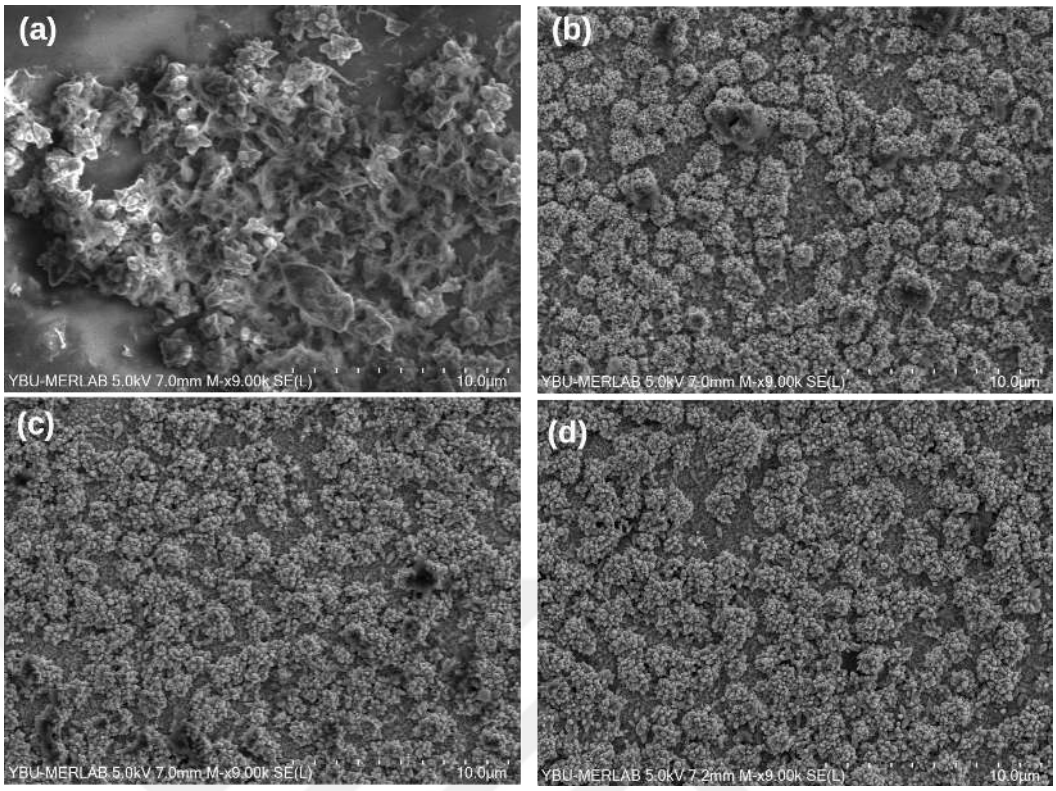

Figure 4.5 (a) FTO/ZnO, (b) FTO/ZnO/Sn-Cu %1, (c) FTO/ZnO/Sn-Cu %2, (d) FTO/ZnO/ Sn-Cu %3, SEM analysis of thin films

4.2 Antimicrobial Activity

According to the results of the analysis, while no zone formation was observed at low metal concentrations, it was determined that both the zone formation and the size of the zone diameter generally increased depending on the increasing concentration. The zone diameters of the bacteria used in the study were shown in Table 4.2.

Table 4.2 The zone diameters (mm) of the bacteria

Metal	***E. coli* ATCC 35218**											
	Concentration (µg/mL)											
	10	25	50	100	250	500	1000	1500	2000	3000	4000	5000
Cu	-	-	-	-	-	-	7.45	8.01	9.78	11.25	11.99	13.09
							±0.02	±0.04	±0.04	±0.02	±0.01	±0.02
Sn	-	-	-	-	-	-	2.50	-	-	-	-	-
							±0.01					
Zn	-	-	-	-	3.47	4.80	7.46	9.42	12.10	13.16	13.73	17.52
					±0.0	±0.2	±0.05	±0.01	±0.01	±0.06	±0.03	±0.01
***S. aureus* ATCC 25923**												
Cu	-	-	-	-	-	-	7.2	10.12	10.13	15.00	15.46	16.94
							±0.01	±0.00	±0.05	±0.03	±0.01	±0.04
Sn	-	-	-	-	-	-	2.60	-	-	-	-	-
							±0.01					
Zn	-	-	-	-	-	-	10.34	10.40	14.79	15.74	16.48	20.38
							±0.01	±0.04	±0.03	±0.03	±0.06	±0.01

*The mean surface area of the inhibitory zone was computed for each, from the mean diameter ± SD.

The highest antimicrobial activity was observed in Zn metal (5000 µg/mL) against S. aureus bacteria, while the lowest activity was observed in Sn metal (1000 µg/mL) against *E. coli* bacteria. Zone diameters against *S. aureus* and *E. coli* bacteria were determined as 20.38 and 2.50 mm, respectively. In both pathogen bacterial strains, it was determined that Zn and Cu metals exhibited the highest antibacterial effect at 5000 µg/mL, the highest concentration used in the study. Zone formation against pathogen

bacteria was observed at 1000 µg/mL of Zn, Cu, and Sn metals, but it was not detected that they did not show any antibacterial effect at higher metal concentrations.

Exhibited zone formation of different concentrations of undoped, ZnO/Sn-Cu %1, ZnO/Sn-Cu %2, and ZnO/Sn-Cu %3 metal against *E. coli* and *S. aureus* were shown in Figure 4.6.

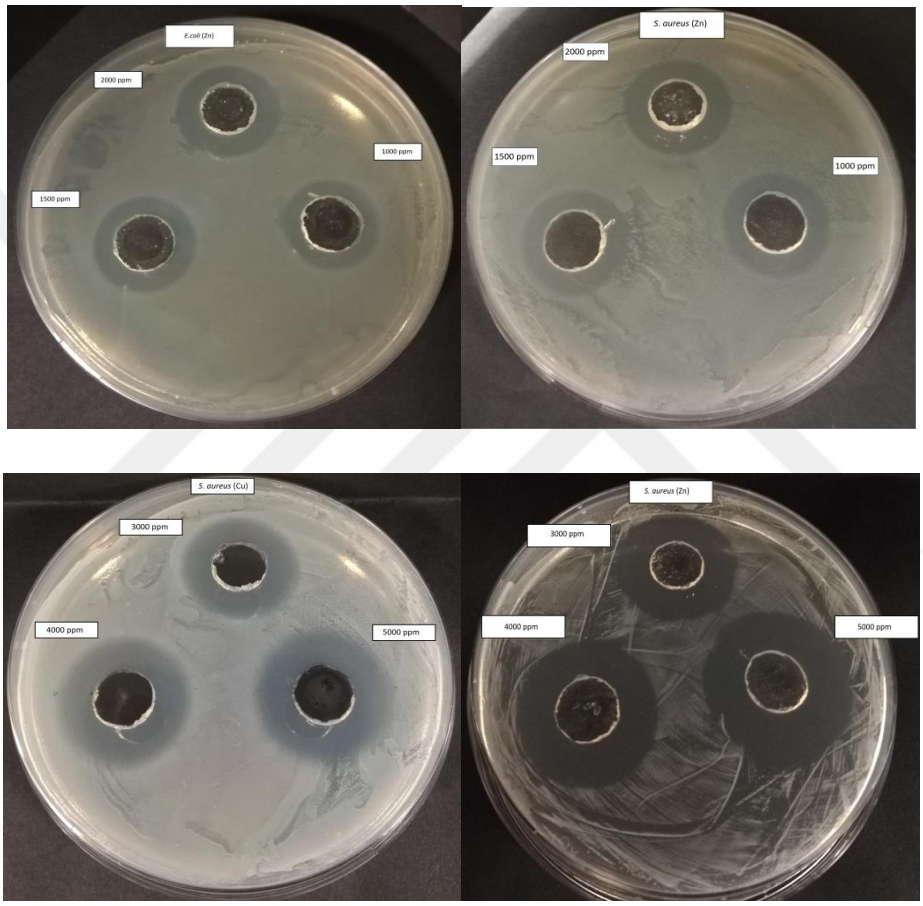

Figure 4.6 Zone formations of undoped, ZnO/Sn-Cu %1, ZnO/Sn-Cu %2, and ZnO/Sn-Cu %3 at different concentrations

Danial *et al.* (2020) synthesized undoped and in-doped (1%, 3%, and 5%) ZnO nanoparticles by sol-gel technique. Antibacterial activities of undoped and in-doped ZnO NPs were determined using the disk diffusion method. The human pathogenic bacteria, two Gram-positive bacteria (*Bacillus subtilis NRRL-B-4219*, and *Staphylococcus aureus ATCC 25923*) and two Gram-negative microorganisms

(*Escherichia coli ATCC 25922* and *Pseudomonas aeruginosa NRRL B23 27853*) were used for antibacterial activity. The zone diameters of the bacteria used in un-doped ZnO and in doped ZnO were determined as 12-15 mm and 12-18 mm, respectively. The highest zone diameter was obtained by *B. subtilis NRRL-B-4219* in 5 % doped ZnO (18 mm) medium.

In another study, the bulk SnO_2 nanoparticles and SnO_2 nanoparticles were tested for antimicrobial activity against to *E. coli ATCC 25922* and *B. subtilis UPMC 1175*. Zone diameter against to E. coli ATCC 25922 was found 3 mm for bulk SnO2 nanoparticles while 5-9 mm for SnO_2 nanoparticles. Zone diameter against to *B. subtilis UPMC 1175* was found 5 mm for bulk SnO_2 nanoparticles while 9 - 22 mm for SnO_2 nanoparticles. The highest antibacterial activity was observed against *B. subtilis UPMC 1175* with the highest inhibition zone of 22 mm (Al-Hada *et al.* 2018).

Ravichandran *et al.* (2016) designated ZnO, copper, and graphene-activated ZnO nanopowders (ZnO:Cu and ZnO:Cu:Graphene) antibacterial activity against E. coli and S. aureus bacteria. According to the results the authors obtained, it was reported that the zone diameters observed in both bacteria were 10 mm for ZnO and ZnO:Cu and 16 mm for ZnO:Cu:Graphene. When we compare our study results with other studies, it is seen that the observed zone diameters for the antimicrobial activity test are larger or similar, that is, the metal powder samples used have higher antibacterial activity values. It is thought that this may be due to the use of different kinds and concentrations of metal powder samples and different pathogen bacteria.

In a second method, in which antimicrobial activities of different metals (undoped, Sn-Cu %1, Sn-Cu %2, and Sn-Cu %3) integrated into glass surfaces were determined against test bacteria, no zone formation was observed around the glass surface.

In El-Kattan *et al.* (2022) study, the antimicrobial activity of curcumin-doped Ag NPs (Cur-Ag NPs) at different concentrations (5, 10, 15, 20, 25 ppm) against pathogenic bacteria isolates (*Staphylococcus aureus MSSA, MRSA, Enterococcus faecalis, Pseudomonas aeruginosa, Klebsiella pneumoniae, Acinetobacter baumannii, Proteus*

vulgaris, and Escherichia coli) was determined and the zone diameters were found among 8.7 - 22.3 mm.

Khan *et al.* (2018) investigated un-doped ZnO and Cu doped ZnO NAPs' (synthesized from aqueous extracts of *Clerodendrum infortunatum* (M1 NAPs) and *Clerodendrum inerme* (M2 NAPs)) antimicrobial activity. Authors reported that both undoped ZnO and Cu-doped ZnO NAPs (M1, NAPs) showed effective antimicrobial activity against *Klebsiella* and *B. subtilis* (13 ± 0.01 and 15 ± 0.03 mm) and (15 ± 0.05 mm and 17 ± 0.11 mm), respectively. Also, they declared that significant antibacterial activity was designated by M2 NAPs against *E. coli* (13 ± 0.09), *S. aureus* (14 ± 0.01), *Klebsiella* (18 ± 0.07), and *B. subtilis* (20 ± 0.10) respectively.

Similar to Khan *et al.* (2018) studies, undoped ZnO_2 and Cu doped ZnO samples were used in our study, but no antibacterial effect was found. The reason for this difference may be due to the fact that the bacterial sources used are different or that the metals integrated into the glass surface are resistant to the pathogens used.

4.3 MIC and MLC/MBC Analysis

Minimum inhibition and minimum lethal concentration of power metals were carried out according to the method specified in 3.1. MIC and MLC results of different concentrations of metals were given in Table 4.3.

Table 4.3 Minimum inhibition and minimum lethal concentration of power metals against *E. coli* and *S. aureus* strains.

Pathogen Bacteria	**Minimum Inhibition Concentration (µg/mL)**		
	Cu	**Sn**	**Zn**
E. coli	800	>5000	400
S. aureus	250	>5000	200
	Minimum Lethal Concentration (µg/mL)		
E. coli	1000	>5000	500
S. aureus	500	>5000	250

As a result of the study, it was observed that the resistance of the pathogens to the metals used varies depending on the metal source and concentration. While the MIC value of *E. coli* bacteria varied between 400>5000 µg/mL, this value was determined as 200>5000 µg/mL in *S. aureus*. MLC values were designated as 500>5000 and 250>5000 µg/mL, respectively. Against *E. coli* bacteria, Zn and Cu metals inhibited bacterial growth at concentrations of 400 and 800 µg/mL and killed bacteria at concentrations of 500 and 1000 µg/mL respectively (Figure 4.7).

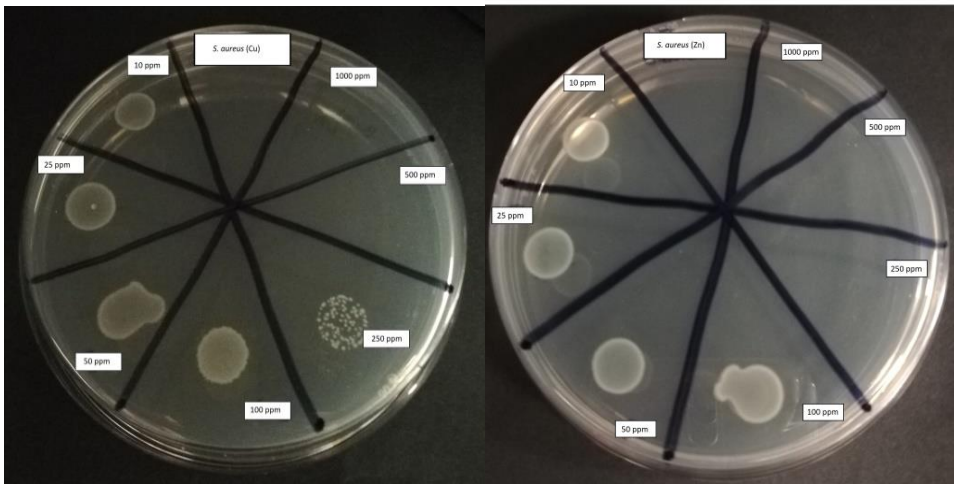

Figure 4.7 MIC and MLC images of undoped, ZnO/Sn-Cu %1, ZnO/Sn-Cu %2, and ZnO/Sn-Cu %3 metals prepared at different concentrations

Khan *et al.* (2018) investigated the Minimum Inhibition Concentration of the antibacterial test of un-doped ZnO and Cu-doped ZnO NAPs (M1 and M2, NAPs) against various bacterial strains (*E. coli*, *S. aureus*, *Klebsiella*, and *B. subtilis*). Authors reported that MIC values for Cu-doped ZnO NAPs (M1 and M2, NAPs) were between 0.03 - 0.95 mg/mL and for un-doped ZnO 0.06 - 1.01 mg/mL.

Seibert *et al.* (2019) determinated the antibacterial activity of ZnO-NPs against important human foodborne pathogens (*Staphylococcus aureus, Salmonella Typhimurium, Bacillus cereus,* and *Pseudomonas aeruginosa*). The authors reported that the Minimum Inhibitory Concentration (MIC) and Minimum Bactericidal Concentration (MBC) were equal to 0.05 mg/mL and 0.5 mg/mL for *S. aureus* and *S. Typhimurium*, respectively.

In another study, in which ZnO, TiO_2, and ZnO-TiO_2 nanoparticles were synthesized by sol-gel method using zinc acetate and titanium isopropoxide, the antifungal properties of nanopowders against Aspergillus flavus were investigated. MIC and MFC values for ZnO, and TiO_2, ZnO-TiO_2 against A. flavus were reported as 156, 78, 39 μg/mL, and 312, 156, 78 μg/mL, respectively (Ilkhechi *et al.* 2021).

4.4 Bacterial Adhesion And Survival Organism Counting

An adhesion test was performed to determine whether *E. coli* ATCC 35218 and *S. aureus* ATCC 25923 pathogenic microorganisms adhered to glass surfaces on which different metals were integrated. To prevent the growth of microorganisms during the adhesion experiments, the studies were carried out in PBS solution. The retention time was carried out as 4 hours. Antimicrobial activities against *E. coli* and *S. aureus* bacteria by survival organism counting method. The number of survival organisms after adhesion and adhesion rates were given in Table 4.4 and Table 4.5.

Table 4.4 Number of survival organisms after adhesion not observed

Number of survival organisms (log_{10})					
Bacteria	ZnO/Sn-Cu %1	ZnO/Sn-Cu %2	ZnO/Sn-Cu %3	Undoped	Control (bacteria)
E. coli	4.77	4.65	4.61	4.55	7.08
S. aureus	4.81	4.79	4.73	4.71	7.55

Table 4.5 Bacterial adhesion on different metal surfaces and undoped surface

Bacterial adhesion (%)		
Metal	***E. coli***	***S. aureus***
ZnO/Sn-Cu %1	67.4	63.7
ZnO/Sn-Cu %2	65.7	63.4
ZnO/Sn-Cu %3	65.1	62.7
Undoped	64.3	62.3

In both bacteria, it was determined that as the metal additive percentage increased in the ZnO/Sn-Cu added samples, there was a decrease in the adhesion percentages of the bacteria. The highest and lowest adhesion rates were determined as ZnO/Sn-Cu %1 (63.7 %) for *E. coli* and *S. aureus*, respectively.

Pathogenic microorganisms were kept on the metal sample integrated on the glass surface for 24 hours and viability counts were made at the end of the incubation period. No viability was observed in any of the glass samples. According to the results of the analysis, it was determined that *E. coli* and *S. aureus* bacteria were able to adhere to the metal samples integrated on the glass surface for 4 hours, but could not survive during the 24-hour waiting period. It is thought that alternative materials can be designed to inhibit or destroy the growth of pathogenic microorganisms with these metals because

of there are no survival pathogenic microorganisms left on the surface and these materials have strong antibacterial and bactericidal effects. However, to reach a definite decision, it is recommended to conduct similar studies with other pathogenic microorganisms.

5. CONCLUSIONS AND RECOMMENDATIONS

ZnO thin films are one of the most widely studied metal oxides in recent years due to both their chemical and physical properties. Because of these features, it is preferred in many fields of optics and electronics. In this thesis, undoped ZnO films and also ZnO thin films with a constant 1% Sn ratio and 1 %, 2 % and 3 % Cu doping ratios, respectively, were produced on FTO substrate by SILAR method. It was aimed to examine the structural, surface morphological, antibacterial and bacterial adhesion and survival organism count characteristics of the produced samples.

SEM Analysis:

When the SEM images of the produced undoped ZnO thin films are examined, it is seen that there is a regional layering and dispersed growth on the FTO surface. It has been observed that as the additive ratios are increased, a regional stratification increases and more uniform and regional agglomerations increase on the FTO surface. In this case, it is observed that the morphological properties of the thin films produced with the additive change significantly depending on the amount of additive.

EDS Analysis:

It was seen that the elements which create the produced films from the EDS analysis were determined. In addition to the expected elements, the presence of impurity atoms such as Na, Mg, Si were also detected.

Antibacterial and Bacterial Analysis:

When the antibacterial activities were examined, it was seen that the produced samples did not show antibacterial activity in other words, the pathogenic microorganisms are resistant to the samples used in the study. It is thought that alternative materials can be designed to inhibit or destroy the growth of pathogenic microorganisms with these

metals because of there are no survival pathogenic microorganisms left on the surface and these materials have strong antibacterial and bactericidal effects. However, to reach a definite decision, it is recommended to conduct similar studies with other pathogenic microorganisms. It was observed that the highest adhesion rate was in the sample with the lowest additive and the highest one is in the 1% Sn-Cu additive.

REFERENCES

Abdelmigid, H. M., Hussien, N. A., Alyamani, A. A., Morsi, M. M., AlSufyani, N. M., & Kadi, H. A. 2022. Green Synthesis of Zinc Oxide Nanoparticles Using Pomegranate Fruit Peel and Solid Coffee Grounds vs. Chemical Method of Synthesis, with Their Biocompatibility and Antibacterial Properties Investigation. Molecules, 27(4): 1236.

Adams, L. K., Lyon, D. Y., & Alvarez, P. J. 2006. Comparative eco-toxicity of nanoscale TiO_2, SiO_2, and ZnO water suspensions. Water research, 40(19): 3527-3532.

Ahmadian, E., Shahi, S., Yazdani, J., Dizaj, S. M., & Sharifi, S. 2018. Local treatment of the dental caries using nanomaterials. Biomedicine & Pharmacotherapy, 108: 443-447.

Ali, D., Butt, M. Z., Muneer, I., Bashir, F., Hanif, M., Khan, T. M., & Abbasi, S. A. 2021. Synthesis, characterization and antibacterial performance of transparent c-axis oriented Al doped ZnO thin films. Surfaces and Interfaces, 27: 101452.

Al-Hada, N. M., Kamari, H. M., Baqer, A. A., Shaari, A. H., Saion, E. 2018. Thermal Calcination-Based Production of SnO_2 Nanopowder: An Analysis of SnO_2 Nanoparticle Characteristics and Antibacterial Activities.Nanomaterialsİ 8(4): 250.

Amendola, V., Amans, D., Ishikawa, Y., Koshizaki, N., Scirè, S., Compagnini, G., ... & Barcikowski, S. 2020. Room-temperature laser synthesis in liquid of oxide, metal-oxide core-shells, and doped oxide nanoparticles. Chemistry-A European Journal, 26(42): 9206-9242.

Blair, J. M., Richmond, G. E., & Piddock, L. J. 2014. Multidrug efflux pumps in Gram-negative bacteria and their role in antibiotic resistance. Future microbiology, 9(10), 1165-1177.

Blair, J., Webber, M. A., Baylay, A. J., Ogbolu, D. O., & Piddock, L. J. 2015. Molecular mechanisms of antibiotic resistance. Nature reviews microbiology, 13(1): 42-51.

Brayner, R., Ferrari-Iliou, R., Brivois, N., Djediat, S., Benedetti, M. F., & Fiévet, F. 2006. Toxicological impact studies based on Escherichia coli bacteria in ultrafine ZnO nanoparticles colloidal medium. Nano letters, 6(4): 866-870.

Bodnar, M., Hartmann, J. F., & Borbely, J. 2005. Preparation and characterization of chitosan-based nanoparticles. Biomacromolecules, 6(5): 2521-2527.

Chua, P. H., Neoh, K. G., Kang, E. T., & Wang, W. 2008. Surface functionalization of titanium with hyaluronic acid/chitosan polyelectrolyte multilayers and RGD for promoting osteoblast functions and inhibiting bacterial adhesion. Biomaterials, 29(10): 1412-1421.

Chinnapaiyan, M., Selvam, Y., Bassyouni, F., Ramu, M., Sakkaraiveeranan, C., Samickannian, A., ... & Abdel-Rehim, M. 2022. Nanotechnology, Green Synthesis and Biological Activity Application of Zinc Oxide Nanoparticles Incorporated Argemone Mxicana Leaf Extract. Molecules, 27(5): 1545.

Christian, P., Von Der Kammer, F., Baalousha, M., & Hofmann, T. 2008. Nanoparticles: Structure, properties, preparation and behaviour in environmental media. Ecotoxicology, 17(5): 326-343.

Collares, F. M., Garcia, I. M., Klein, M., Parolo, C. F., Sánchez, F. A. L., Takimi, A., ... & Leitune, V. C. 2020. Exploring Needle-Like Zinc Oxide Nanostructures for Improving Dental Resin Sealers: Design and Evaluation of Antibacterial, Physical and Chemical Properties. Polymers, 12(4): 789.

Davies, J., & Davies, D. 2010. Resistance origins and evolution of antibiotic. Microbiology and Molecular Biology reviews. Microbiol Mol Biol Rev, 74(3): 417-33.

Danial, E. N., Hjiri, M., Abdel-Wahab, M. S., Alonizan, N. H., El Mir, L., & Aida, M. S. 2020. Antibacterial activity of In-doped ZnO nanoparticles. Inorganic Chemistry Communications, 122: 108281.

Doyle, M. E. 2006. Nanotechnology: a brief literature review. Food Research Institute, UW-Madison.

El-Kattan, N., Emam, A. N., Mansour, A. S., Ibrahim, M. A., Abd El-Razik, A. B., Allam, K. A., ... & Ibrahim, S. A. 2022. Curcumin assisted green synthesis of silver and zinc oxide nanostructures and their antibacterial activity against some

clinical pathogenic multi-drug resistant bacteria. RSC advances, 12(28): 18022-18038.

Elster, C., Fourest, E., Baudin, F., Larsen, K., Cusack, S., & Ruigrok, R. W. 1994. A small percentage of influenza virus M1 protein contains zinc but zinc does not influence in vitro M1-RNA interaction. Journal of General Virology, 75(1): 37-42.

Ferblantier, G., Mailly, F., Al Asmar, R., Foucaran, A., & Pascal-Delannoy, F. 2005. Deposition of zinc oxide thin films for application in bulk acoustic wave resonator. Sensors and Actuators A: Physical, 122(2): 184-188.

Goncharova, D., Gavrilenko, E., Nemoykina, A., & Svetlichnyi, V. 2018. Antibacterial activity of zinc oxide nanoparticles obtained by pulsed laser ablation in water and air. In MATEC Web of Conferences, pp. 237-243, EDP Sciences.

Göpel, W., Pollmann, J., Ivanov, I., & Reihl, B. 1982. Angle-resolved photoemission from polar and nonpolar zinc oxide surfaces. Physical Review B, 26(6): 3144.

Heinlaan, M., Ivask, A., Blinova, I., Dubourguier, H. C., & Kahru, A. 2008. Toxicity of nanosized and bulk ZnO, CuO and TiO_2 to bacteria Vibrio fischeri and crustaceans Daphnia magna and Thamnocephalus platyurus. Chemosphere, 71(7): 1308-1316.

Husain, F. M., Qais, F. A., Ahmad, I., Hakeem, M. J., Baig, M. H., Masood Khan, J., & Al-Shabib, N. A. 2022. Biosynthesized zinc oxide nanoparticles disrupt established biofilms of pathogenic bacteria. Applied Sciences, 12(2): 710.

Hussain, S. 2008. Investigation of structural and optical properties of nanocrystalline ZnO.

Ilkhechi, N. N., Mozammel, M., & Khosroushahi, A. Y. 2021. Antifungal effects of ZnO, TiO_2 and ZnO-TiO_2 nanostructures on Aspergillus flavus. Pesticide Biochemistry and Physiology, 176: 104869.

Islam, F., Shohag, S., Uddin, M. J., Islam, M. R., Nafady, M. H., Akter, A., ... & Cavalu, S. 2022. Exploring the Journey of Zinc Oxide Nanoparticles (ZnO-NPs) toward Biomedical Applications. Materials, 15(6): 2160.

Jiang, Y., Zhang, L., Wen, D., & Ding, Y. 2016. Role of physical and chemical interactions in the antibacterial behavior of ZnO nanoparticles against E. coli. Materials Science and Engineering: C, 69: 1361-1366.

Kahru, A., Ivask, A., Kasemets, K., Pollumaa, L., Kurvet, I., François, M., & Dubourguier, H. C. 2005. Biotests and biosensors in ecotoxicological risk assessment of field soils polluted with zinc, lead, and cadmium. Environmental Toxicology and Chemistry: An International Journal, 24(11): 2973-2982.

Kelly, K. A., Havrilla, C. M., Brady, T. C., Abramo, K. H., & Levin, E. D. 1998. Oxidative stress in toxicology: established mammalian and emerging piscine model systems. Environmental health perspectives, 106(7): 375-384.

Khan, I., Saeed, K., & Khan, I. 2019. Nanoparticles: Properties, applications and toxicities. Arabian Journal of Chemistry, 12(7): 908-931.

Khan, S. A., Noreen, F., Kanwal, S., Iqbal, A., & Hussain, G. 2018. Green synthesis of ZnO and Cu-doped ZnO nanoparticles from leaf extracts of Abutilon indicum, Clerodendrum infortunatum, Clerodendrum inerme and investigation of their biological and photocatalytic activities. Materials Science and Engineering: C, 82: 46-59.

Klapiszewska, I., Kubiak, A., Parus, A., Janczarek, M., & Ślosarczyk, A. 2022. The in Situ Hydrothermal and Microwave Syntheses of Zinc Oxides for Functional Cement Composites. Materials, 15(3): 1069.

Kumar, A., & Schweizer, H. P. 2005. Bacterial resistance to antibiotics: active efflux and reduced uptake. Advanced drug delivery reviews, 57(10): 1486-1513.

Lee, S. P., Xiao, J., Knutson, J. R., Lewis, M. S., & Han, M. K. 1997. Zn^{2+} promotes the self-association of human immunodeficiency virus type-1 integrase in vitro. Biochemistry, 36(1): 173-180.

Llama-Palacios, A., Sánchez, M. C., Díaz, L. A., Cabal, B., Suárez, M., Moya, J. S., ... & Herrera, D. 2019. In vitro biofilm formation on different ceramic biomaterial surfaces: Coating with two bactericidal glasses. Dental Materials, 35(6): 883-892.

Long, T. C., Saleh, N., Tilton, R. D., Lowry, G. V., & Veronesi, B. 2006. Titanium dioxide (P25) produces reactive oxygen species in immortalized brain microglia

(BV2): implications for nanoparticle neurotoxicity. Environmental science & technology, 40(14): 4346-4352.

Mann, S., Burkett, S. L., Davis, S. A., Fowler, C. E., Mendelson, N. H., Sims, S. D., ... & Whilton, N. T. 1997. Sol-gel synthesis of organized matter. Chemistry of materials, 9(11): 2300-2310.

Mashaghi, S., Jadidi, T., Koenderink, G., & Mashaghi, A. 2013. Lipid nanotechnology. International journal of molecular sciences, 14(2): 4242-4282.

Mohd Yusof, H., Mohamad, R., Zaidan, U. H., & Rahman, A. 2019. Microbial synthesis of zinc oxide nanoparticles and their potential application as an antimicrobial agent and a feed supplement in animal industry: a review. Journal of animal science and biotechnology, 10(1): 1-22.

Nicolau, Y. F. 1985. Solution deposition of thin solid compound films by a successive ionic-layer adsorption and reaction process. Applications of Surface Science, 22: 1061-1074.

Özgür, Ü., Alivov, Y. I., Liu, C., Teke, A., Reshchikov, M., Doğan, S., ... & Morkoç, A. H. 2005. A comprehensive review of ZnO materials and devices. Journal of applied physics, 98(4): 11.

Park, C. H., Zhang, S. B., & Wei, S. H. 2002. Origin of p-type doping difficulty in ZnO: The impurity perspective. Physical Review B, 66(7): 073202.

Patra, J. K., Das, G., Fraceto, L. F., Campos, E. V. R., Rodriguez-Torres, M. D. P., Acosta-Torres, L. S., ... & Shin, H. S. 2018. Nano based drug delivery systems: recent developments and future prospects. Journal of nanobiotechnology, 16(1): 1-33.

Pati, R., Mehta, R. K., Mohanty, S., Padhi, A., Sengupta, M., Vaseeharan, B., ... & S onawane, A. 2014. Topical application of zinc oxide nanoparticles reduces bacterial skin infection in mice and exhibits antibacterial activity by inducing oxidative stress response and cell membrane disintegration in macrophages. Nanomedicine: Nanotechnology, Biology and Medicine, 10(6):1195-1208.

Premanathan, M., Karthikeyan, K., Jeyasubramanian, K., & Manivannan, G. 2011. Selective toxicity of ZnO nanoparticles toward Gram-positive bacteria and cancer cells by apoptosis through lipid peroxidation. Nanomedicine: Nanotechnology, Biology and Medicine, 7(2): 184-192.

Qi, Z., Cao, H., Jiang, H., Zhao, J., & Tang, Z. 2016. Combinations of bacterial species associated with symptomatic endodontic infections in a Chinese population. International Endodontic Journal, 49(1): 17-25.

Randall, C. P., Mariner, K. R., Chopra, I., & O'Neill, A. J. 2013. The target of daptomycin is absent from Escherichia coli and other gram-negative pathogens. Antimicrobial agents and chemotherapy, 57(1): 637-639.

Ramesh, S., Ramaclus, J. V., Mosquera, E., & Das, B. B. 2016. Sol-gel synthesis, structural, optical and magnetic characterization of Ag 3 (2+ x) Pr x Nb 4− x O 11+ δ (0.0≤ x≤ 1.0) nanoparticles. RSC Advances, 6(8): 6336-6341.

Ravichandran, K., Chidhambaram, N., & Gobalakrishnan, S. 2016. Copper and Graphene activated ZnO nanopowders for enhanced photocatalytic and antibacterial activities. Journal of Physics and Chemistry of Solids, 93: 82-90.

Reygaert, W. C. 2018. Department of Biomedical Sciences, Oakland University William Beaumont School of Medicine, Rochester, MI, USA, An overview of the antimicrobial resistance mechanisms of bacteria. AIMS Microbiol, 4: 482-501.

Reygaert, W. 2009. Methicillin-resistant Staphylococcus aureus (MRSA): molecular aspects of antimicrobial resistance and virulence. Clinical Laboratory Science, 22(2): 115.

Rikans, L. E., & Hornbrook, K. R. 1997. Lipid peroxidation, antioxidant protection and aging. Biochimica et Biophysica Acta (BBA)-Molecular Basis of Disease, 1362(2-3): 116-127.

Ristov, M., Sinadinovski, G. J., & Grozdanov, I. 1985. Chemical deposition of Cu_2O thin films. thin solid films, 123(1): 63-67.

Shankar Ganesh, A., Subramani, S., Anandh, B., & Sakthivel, R. 2022. analyzıng antımıcrobıal actıvıty of aluminium doped zno thın fılms. Rasayan J. Chem, 15(1): 387-394.

Sharma, R., Kumar, S., Singh, P., & Kapila, S. 2020. Structural, Morphological and Antimicrobial Study of ZnO/Ag Nanoparticles. Biomedical and Pharmacology Journal, 13(4): 1645-1652.

Sheeparamatti, B. G., Sheeparamatti, R. B., & Kadadevaramath, J. S. 2007. Nanotechnology: Inspiration from nature. IETE Technical Review, 24(1): 5-8.

Seibert, J. B., Bautista-Silva, J. P., Amparo, T. R., Petit, A., Pervier, P., dos Santos Almeida, J. C., ... & Dos Santos, O. D. H. 2019. Development of propolis nanoemulsion with antioxidant and antimicrobial activity for use as a potential natural preservative. Food chemistry, 287: 61-67.

Stoimenov, P. K., Klinger, R. L., Marchin, G. L., & Klabunde, K. J. 2002. Metal oxide nanoparticles as bactericidal agents. Langmuir, 18(17): 6679-6686.

Song, W., & Ge, S. 2019. Application of antimicrobial nanoparticles in dentistry. Molecules, 24(6): 1033.

Taniguchi, N. 1994. 1993 ASPE distinguished lecturer. Precision Engineering, 16(1), 5-24.

Thevenot, D. R., Toth, K., Durst, R. A., & Wilson, G. S. 1999. Electrochemical biosensors: recommended definitions and classification. Pure and applied chemistry, 71(12): 2333-2348.

Tülü, G., Kaya, B. Ü., Çetin, E. S., & Köle, M. 2021. Antibacterial effect of silver nanoparticles mixed with calcium hydroxide or chlorhexidine on multispecies biofilms. Odontology, 109(4): 802-811.

Vartiainen, J., Rättö, M., Tapper, U., Paulussen, S., & Hurme, E. 2005. Surface modification of atmospheric plasma activated BOPP by immobilizing chitosan. Polymer Bulletin, 54(4): 343-352.

Yang, Y., Xu, Z., Guo, Y., Zhang, H., Qiu, Y., Li, J., ... & Fan, Z. 2021. Novel core–shell CHX/ACP nanoparticles effectively improve the mechanical, antibacterial and remineralized properties of the dental resin composite. Dental Materials, 37(4): 636-647.

Waseda, Y., Matsubara, E., & Shinoda, K. 2011. X-ray diffraction crystallography: introduction, examples and solved problems. Springer Science & Business Media.

World Health Organization. Global action plan on antimicrobial resistance. Geneva, Switzerland: WHO, 2015.

Zhang, L., Jiang, Y., Ding, Y., Povey, M., & York, D. 2007. Investigation into the antibacterial behaviour of suspensions of ZnO nanoparticles (ZnO nanofluids). Journal of Nanoparticle Research, 9(3): 479-489.